



HAL
open science

Enhanced heat transfer in shell-side condensation

André Bontemps, Mourad Belghazi

► **To cite this version:**

André Bontemps, Mourad Belghazi. Enhanced heat transfer in shell-side condensation. International journal of heat exchangers, 2002, 3 (2), pp.201-239. hal-00184109

HAL Id: hal-00184109

<https://hal.science/hal-00184109>

Submitted on 7 Feb 2020

HAL is a multi-disciplinary open access archive for the deposit and dissemination of scientific research documents, whether they are published or not. The documents may come from teaching and research institutions in France or abroad, or from public or private research centers.

L'archive ouverte pluridisciplinaire **HAL**, est destinée au dépôt et à la diffusion de documents scientifiques de niveau recherche, publiés ou non, émanant des établissements d'enseignement et de recherche français ou étrangers, des laboratoires publics ou privés.

Enhanced Heat Transfer in Shell-Side Condensation

André Bontemps* and Mourad Belghazi

Université Joseph Fourier
LEGI/GRETh CEA Grenoble, France

INTRODUCTION

The typical example of a non-compact heat exchanger is the shell-and-tube type. However, many attempts have been made to increase the compactness of such heat exchangers. Among these are the use of enhanced surface tubes in order to replace the smooth tubes still used. This paper describes the evolution of experimental observations and reviews the main models available in the literature for predicting the shell-side heat transfer coefficients for single tubes and tube bundles for pure fluids and azeotropic mixtures and for non-azeotropic mixtures.

In the case of condensation of pure fluids, heat transfer is controlled by the thermal resistance of the condensate film. The augmentation of condensation heat transfer can be achieved through thinning the condensate film. This can be obtained by draining the condensate via gravity, surface tension or, more rarely, electrical or other mechanical forces. Another way is to augment turbulent mixing of the condensate. In the case of mixtures, a supplementary resistance appears which is produced by the accumulation near the liquid-vapour interface of a layer of the more volatile vapour whose condensation rate is lower than those of the other vapours. This resistance controls condensation heat transfer in most cases and the ways to augment heat transfer should be different.

A large number of specifically designed enhanced surface tubes have been tested to find the best surface geometry for condensing either pure fluid or vapour mixture. These surfaces can be classified in three types: one-dimensional (1-D) surfaces (smooth tubes), two-dimensional (2-D) surfaces (with transverse plain fins) and three-dimensional (3-D) surfaces (with interrupted fins, spines, wires, etc...). The 2-D and 3-D surfaces allow the surface tension effects to be enhanced. Moreover, other enhancement techniques can be employed by using promoting systems attached to the tubes such as drainage strips or external systems such as electric fields.

In this paper, main results concerning condensation heat transfer at the outside of smooth tubes are recalled to serve as a reference. Then, main experimental results and theoretical methods of performance prediction are presented and discussed for 2-D surface tubes. Finally, some results and theoretical models are presented for 3-D surface tubes and comparison is made with 2-D surfaces. Several relevant reviews have already been presented by many authors. One can cite Marto (1984) for smooth tubes and heat transfer augmentation techniques and Marto (1988) for smooth or integral-fin and enhanced surface tubes, Webb (1988), Sukhatme (1990) and more recently, Browne and Bansal (1999). The role of surface tension was emphasised by Shah et al. (1999) and Yang (1999). A statistical review was carried out by Rifert (1998) in which are included the basic principles of models as well as the dynamic of the published works from 1947 to 1997. Whilst the effects of the vapour velocity will not be considered here it is useful to mention the paper of Cavallini et al. (1996) which is, to our knowledge, the only work which looks at the effects of vapour velocity on condensation on integral-fin tubes. However, these reviews concerned essentially condensation of pure vapours. For this reason, special attention will be paid to vapour mixtures of which few results have been published in the literature.

1. PURE FLUIDS

1.1 Single horizontal smooth tubes

The early film condensation analysis for a horizontal smooth tube was carried out by Nusselt (1916), with the following hypotheses: heat transfer in the liquid film restricted to conduction, pure vapour at saturation temperature T_{sat} , wall temperature T_w uniform and no shear at liquid-vapour interface. Neglecting momentum effects, a balance of the shear, gravity and pressure forces leads to the classical expression of the average heat transfer coefficient:

$$\alpha_{Nu} = 0.728 \left(\frac{g \rho_l (\rho_l - \rho_v) \lambda_l^3 \Delta h_{lv}}{D \mu_l (T_{sat} - T_w)} \right)^{1/4} \quad (1)$$

where ρ_l and ρ_v are the liquid and vapour density respectively, μ_l the liquid dynamic viscosity, λ_l the liquid thermal conductivity and Δh_{lv} the latent heat of condensation.

Defining the Nusselt number Nu by:

$$Nu = \frac{\alpha D}{\lambda_l} \quad (2)$$

formula (1) can be written by using dimensionless numbers, as

$$Nu_{Nu} = 0.728 \left(\frac{Ga Pr_l}{Ph} \right)^{1/4} \quad (3)$$

where Ga is a Galileo number defined by

$$Ga = \frac{g (\rho_l - \rho_v) Pr_l D^3}{\rho_l \nu_l^2} \quad (4)$$

Pr_l the liquid Prandtl number

$$Pr_l = \frac{\mu_l c_{pl}}{\lambda_l} \quad (5)$$

and Ph the phase change number:

$$Ph = \frac{c_{pl}(T_{sat} - T_w)}{\Delta h_{lv}} \quad (6)$$

The other way is to define a Nusselt number independently of geometry (also called condensation number) by writing

$$Nu^* = \frac{\alpha}{\lambda_l} \left[\frac{\mu_l^2}{\rho_l (\rho_l - \rho_v) g} \right]^{1/3} \quad (7)$$

and the condensate Reynolds number Re_l as

$$Re_l = \frac{4 \Gamma}{\mu_l} \quad (8)$$

where Γ is the lineic condensate mass flow. With these notations, the Nusselt theory gives:

$$Nu^* = 1.52 Re_l^{1/3} \quad (9)$$

or by using the above defined dimensionless numbers:

$$Nu^* = 0.728 \left[\frac{Pr_l}{Ga^{1/3} Ph} \right]^{1/4} \quad (10)$$

Numerous studies followed the pioneering work of Nusselt accounting for condensate subcooling (Rohsenow, 1956), vapour superheating, inertial forces (Sparrow & Gregg, 1959) and shear stress. Nevertheless, the Nusselt formula remains as a standard to calculate the heat transfer coefficient when the vapour is stagnant. Note that this formula was

established by assuming the fluid thermophysical properties to be constant and taken at the saturation temperature. It is accepted now that the fluid properties are to be taken at a characteristic temperature which is often chosen as the arithmetic average T_f between the wall temperature T_w and the saturation temperature T_{sat} .

$$T_f = \frac{T_w + T_{sat}}{2} \quad (11)$$

A difference up to 10 % may be observed when using different characteristic temperatures (Figure 1).

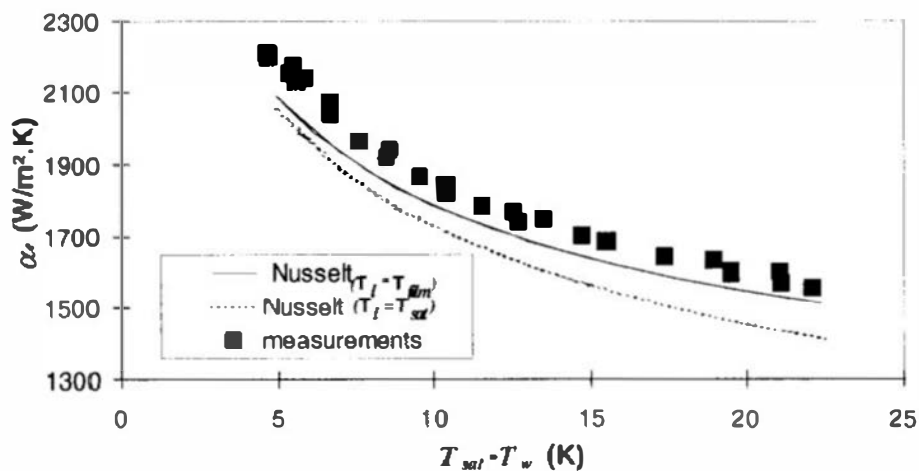


FIGURE 1. Influence of fluid characteristic temperatures on theoretical values of the heat transfer coefficient (After Belghazi, 2001).

Other characteristic temperatures can be used, in particular if condensate subcooling is taken into account.

1.2 Smooth tube bundle

With the same assumptions as in the case of a single tube, Nusselt analysed condensation on horizontal banks of smooth tubes. He assumed all the condensate dropping from any tube falls on the next lower tube. He found that the heat transfer coefficient averaged over all n tubes in a vertical bank is given by:

$$\bar{\alpha}_n = 0.728 \left(\frac{g \rho_l (\rho_l - \rho_v) \lambda_l^3 \Delta h_{lv}}{n D \mu_l (T_{sat} - T_w)} \right)^{1/4} \quad (12)$$

or

$$\frac{\bar{\alpha}_n}{\alpha_l} = n^{-1/4} \quad (13)$$

α_j being the heat transfer coefficient of the top tube. The experimental data for banks of tubes falling above the values of the equation (13), Collier and Thome (1994). Kern (1965) proposed to adapt this formula by modifying the 1/4 exponent to take into account the difference between actual phenomena (ripples, etc...) and ideal model of Nusselt. This led to a family of correlations of the form:

$$\frac{\bar{\alpha}_n}{\alpha_1} = n^{-\gamma} \quad (14)$$

$\gamma = 1/6$ being the value proposed by Kern. For the j^{th} tube, one obtains the following relation:

$$\frac{\alpha_j}{\alpha_1} = j^{1-\gamma} - (j-1)^{1-\gamma} \quad (15)$$

This modification does not account for the dependence of α_j on the heat flux or on the temperature difference $T_{sat} - T_w$. Chen (1961) suggested that since the condensate is subcooled, further condensation can occur on the liquid falling from one tube to the other. Assuming all the cooling energy is removed and considering the additional effect of the momentum gain, he found the following result:

$$\bar{\alpha}_n = 0.728 \left(\frac{g \rho_l (\rho_l - \rho_v) \lambda_l^3 \Delta h_{lv}}{n D \mu_l (T_{sat} - T_w)} \right)^{1/4} \left(1 + 0.2 (n-1) \frac{c_{pl} (T_{sat} - T_w)}{\Delta h_{lv}} \right) \quad (16)$$

with the condition that

$$(n-1) \frac{c_{pl} (T_{sat} - T_w)}{\Delta h_{lv}} < 2$$

This equation agrees reasonably well with experimental data. It has been shown that using the Chen suggestion with the Kern exponent allows the two phenomena of ripples and subcooled falling condensate to be taken into account and to obtain a better agreement (Belghazi et al., 2001) (Figure 2)

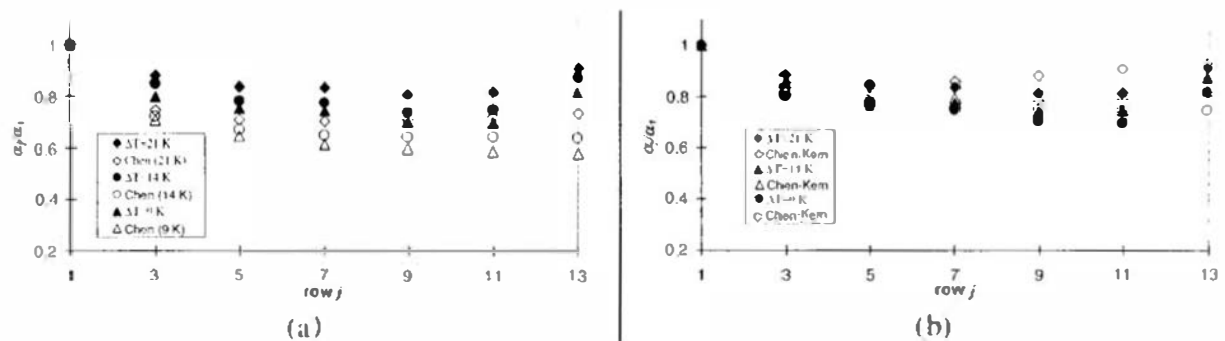


FIGURE 2. Variation of the ratio between the heat transfer coefficient of the j th row and the heat transfer coefficient of the first row as a function of the row number. (a) Comparison experimental results and Chen et al. model. (b) Comparison experimental results and modified Chen et al. model.

1.3 Single integral-fin tubes (2-D)

The basic surface extension is the low-fin 2-D geometry. These fins are either rectangular or trapezoidal and the fin density can vary from 433 fins per meter (fpm) or 11 fins per inch (fpi) to 1640 fpm. (42 fpi). Other 2-D geometries were used whose most common are given in figure 3.

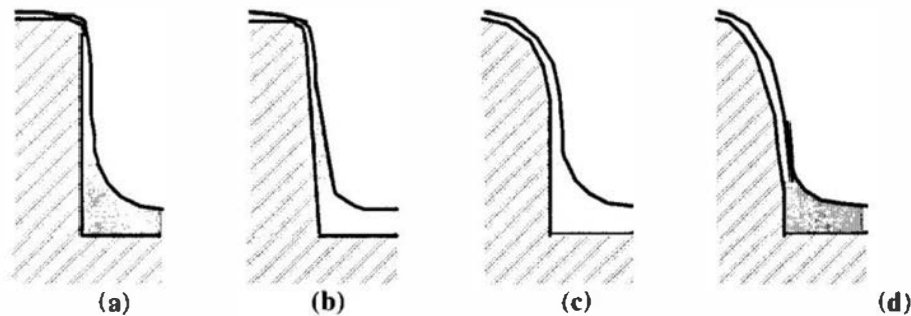


FIGURE 3. Fin profiles in 2-D geometries: (a) Rectangular fin. (b) Trapezoidal fin. (c) Curved profile and rectangular part. (c) Curved profile.

The effect of the fins is to drain the condensate either by gravity or by surface tension effects, improving the heat transfer coefficient. However surface tension effects are also responsible for condensate retention or flooding between the fins in the lower part of tubes which deteriorate the heat transfer coefficient (Figure 4). The resulting coefficient is a compromise between these two effects.

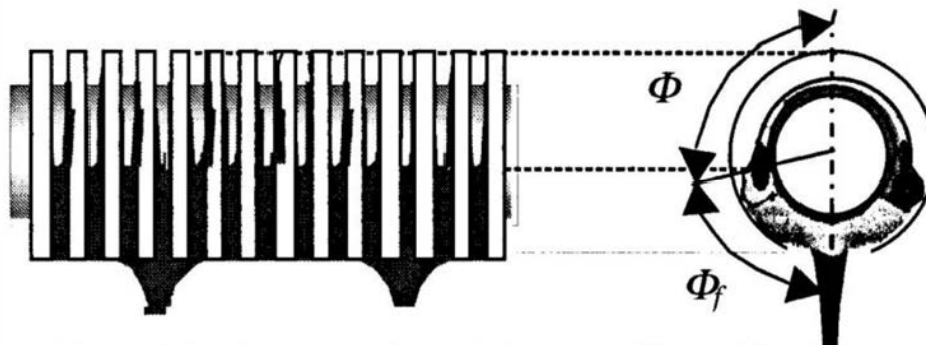


FIGURE 4. Condensate retention at the lower part of integral-fin tubes.

1.3.1 Gravity drainage models

The first model to analyse the condensation on rectangular fins was developed by Beatty and Katz (1948). These authors neglected surface tension forces and considered a Nusselt-type condensation on a vertical plate (fin flanks) and on horizontal tubes (fin tips and space between fins). The heat transfer coefficient can be written as

$$\alpha_{BK} = \frac{l}{\eta} \left[\frac{A_r}{A} \alpha_H + \frac{\eta_f A_f}{A} \alpha_P \right] \quad (17)$$

where α_H and α_P are the heat transfer coefficients given by Nusselt for horizontal tube and vertical plate respectively and where A_f and A_r are the surfaces of the fin flanks and of the tube parts between the fins respectively. The total surface is

$$A = A_r + A_f$$

η is the surface efficiency (taken as 1 by Beatty and Katz) and η_f the fin efficiency.

This heat transfer coefficient can be written under the classical form:

$$\alpha_{BK} = 0.689 \left(\frac{Ga Pr \eta}{Ph} \right)^{1/4} \left(\frac{l}{D_{eq}} \right)^{1/4} \frac{l}{\eta} \quad (18)$$

where the equivalent diameter is defined as

$$\left(\frac{l}{D_{eq}} \right)^{1/4} = 1.3 \eta_f \left(\frac{A_f}{A} \right) \left(\frac{l}{e_{eq}^{1/4}} \right) + \left(\frac{A_r}{A} \right) \left(\frac{l}{D_r^{1/4}} \right) \quad (19)$$

and where e_{eq} is an equivalent fin height

$$e_{eq} = \pi \left(\frac{D_e^2 \cdot D_r^2}{4 D_e} \right) \quad (20)$$

In the above formulae, D_e and D_r are the diameters at the fin tip and at the fin root respectively (Figure 5).

The Beatty and Katz formula was improved by Smirnov and Lukanov (1972) to account for fin tips, the formula is unchanged if using the new equivalent diameter:

$$\left(\frac{l}{D_{eq}} \right)^{1/4} = 1.3 \eta_f \left(\frac{A_f}{A_{eq}} \right) \left(\frac{l}{e_{eq}^{1/4}} \right) + \left(\frac{A_t}{A_{eq}} \right) \left(\frac{l}{D_e^{1/4}} \right) + \left(\frac{A_r}{A_{eq}} \right) \left(\frac{l}{D_r^{1/4}} \right) \quad (21)$$

A_f , A_t and A_r being the area of the fin flanks, the fin tip and the space between the fins respectively and where

$$A_{eq} = \eta_f (A_f + A_t) + A_r \quad (22)$$

These equations fit reasonably well the data from low surface tension fluids such as refrigerants with low fin density tubes. For other fluids and other finned tubes the surface tension effects cannot be neglected.

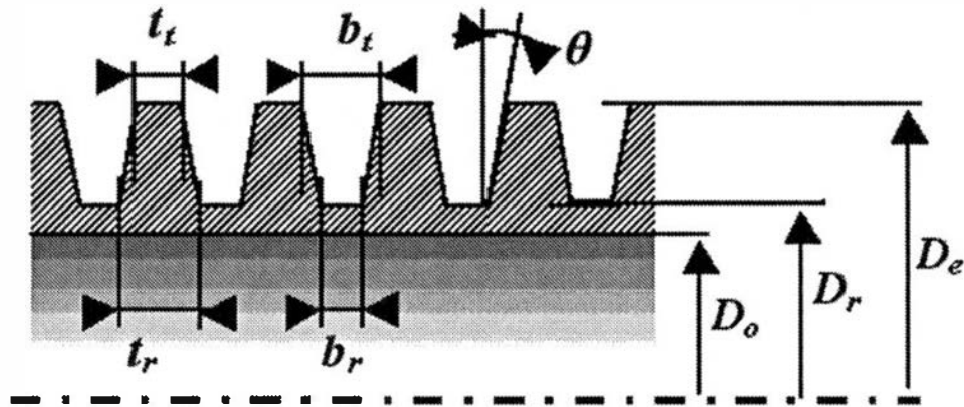


FIGURE 5. Definition of geometrical parameters in a tube with trapezoidal fins.

1.3.2. Surface tension effects

a - Retention angle Several authors (see for instance Rudy and Webb (1985), Masuda and Rose (1987)) have calculated and/or measured the angle Φ_f of the liquid rise height between the fins. The widely accepted value is that calculated by Honda et al. (1983) who developed an approximate expression for the unflooded angle Φ :

$$\Phi = \cos^{-1} \left[\left(\frac{4 \sigma \cos \theta}{\rho_l g b_t D_e} \right) - 1 \right] \text{ with } e > b_t/2 \quad (23)$$

Moreover, Masuda and Rose (1987), by observing static liquid retention have shown that the liquid can be retained on the upper part of the tube (unflooded region) at the boundary of the fin flank and of the tube surface.

b - Heat transfer coefficient The most simplest method to account for condensate retention by surface tension forces is to use the Beatty and Katz theory by subtracting the submerged part of a tube.

In their model, Beatty and Katz do not take into account explicitly the flooding of the lower part of the finned tube. However, the coefficient 0.689 in place to 0.728 has been obtained by fitting experimental results for condensation of 6 fluids on a low fin density tube. Butrymowicz and Trela (1997) consider that such a modification is the consequence of condensate retention allowing the flooding angle to be determined as

$$\Phi_f = \frac{0.689}{0.728}$$

Such a constant value is not in agreement with the theoretical results. A first attempt to account for the variable flooded region was made by Rudy and Webb (1981) in assuming that only the unflooded region is active. They wrote

$$\alpha = \alpha_{BK} \frac{\Phi}{\pi} = \alpha_{BK} \left(1 - \frac{\Phi_f}{\pi} \right) = \alpha_{BK} (1 - C_b) \quad (24)$$

where C_b is the fraction of the tube which retains the condensate. The authors found that this equation underpredicted their experimental results and postulated that other mechanisms occurred to drain the condensate.

Another approach is to account for the retention effect by doing a weighted average of the heat transfer coefficients for the flooded and the unflooded region. Sardesai et al. (1982) and Owen et al. (1983) proposed an extension to the Beatty and Katz model and expressed the average heat transfer coefficient as:

$$\alpha_O = (1 - C_b) \alpha_{BK} + C_b \alpha_b \quad (25)$$

or under the form:

$$Nu^* = 0.728 \left(\frac{Pr_l}{Ga^{1/3} Ph} \right)^{1/4} \left[\left(\frac{D_e}{D_{eq}} \right)^{1/4} (1 - C_b) + \left(\frac{D_e}{D_r} \right)^{1/4} C_b \right] \quad (26)$$

where α_b is the heat transfer coefficient in the flooded zone calculated from usual correlations for single phase flow. However, these authors found also that this method underpredicted the experimental results.

Webb et al. (1985) developed a theoretical model which assumes that (i) equation (17) applied only for the unflooded fraction and (ii) the heat transfer coefficient on the fin flanks α_f is established by assuming that surface tension is the dominant force in condensate drainage from the fin surface. They proposed the equation:

$$\alpha \eta = (1 - C_b) \left(\alpha_H \frac{A_r}{A} + \eta_f \alpha_f \frac{A_f + A_l}{A} \right) + C_b \alpha_b \quad (27)$$

where α_H is the heat transfer coefficient on the unflooded root surface of the tube between fins. The determination of α_f is made by using the method of Adamek (1981) who describes the curvature of the surface condensate with a function depending on an exponent ζ whose exact value is difficult to know. They found that their model predicted their experimental data for R-11 to within $\pm 20\%$ and Wanniarachchi et al. (1986) found that their experimental data for steam were predicted within about $\pm 20\%$ except for completely flooded tubes.

The most complete but complex method was developed by Honda and Nozue (1987) to predict the average heat transfer coefficient for film condensation on horizontal tubes with trapezoidal fins. In their model, the tube is divided in flooded and unflooded region (Figure 6). On the fin surface, the authors assume that the condensate is drained by surface tension and gravity and that in the interfin space the condensate is drained only by

gravity. They solve numerically the equation for the condensate film thickness and, based on their numerical results, they give an approximate expression for the Nusselt numbers in both the unflooded (Nu_{du}) and flooded (Nu_{df}) regions. They finally give the average heat transfer coefficient under the form:

$$Nu_{HN} = \frac{\alpha_{HN} D_e}{\lambda_l} = \frac{Nu_{du} \lambda_u (1 - \bar{T}_{wu}) + Nu_{df} \eta_f (1 - \bar{T}_{wf})}{(1 - \bar{T}_{wu})(1 - C_b) + (1 - \bar{T}_{wf})C_b} \quad (28)$$

where η is the fin efficiency, \bar{T}_{wu} and \bar{T}_{wf} are the dimensionless wall temperatures in the unflooded and flooded zones respectively. In the model are included the wall temperature variations determined by an iterative procedure. The model predicts the experimental results of various investigators within $\pm 20\%$. A further extension of this analysis by Honda et al. (1987) reduced the prediction to within $\pm 10\%$.

Another model was presented by Adamek and Webb (1990) for predicting the heat transfer coefficient for condensation on tubes with trapezoidal or rectangular fins. In their model, the tube surface is divided in 3 regions: unflooded, flooded and drop-off zones. This last zone, where a condensate drop is formed, insulates the fin tips. The heat transfer in this zone, estimated to represent 10% of the tube circumference, was neglected. The average heat transfer coefficient is given by:

$$\alpha_{AW} = \frac{4 N_f L_{ech} \Delta h_{lv}}{A \Delta T} (\dot{m}_{unflooded} + \dot{m}_{flooded}) \quad (29)$$

where N_f is the number of fins per meter, L_{ech} the tube length and A the heat exchange surface area. The mass flow rate $\dot{m}_{unflooded}$ is determined by adding the contributions of the different parts of a fin in the unflooded region. The mass flow rate $\dot{m}_{flooded}$ is given by the condensate formed on the fin tip which is considered as the only active part in the flooded region. This model is rather easily usable since it does not need a iterative procedure. It was tested with 7 fluids and 80 different tube geometries and predicted the experimental results to within $\pm 15\%$ for most of them.

More recently, Sreepathi et al. (1996) have developed a generalised correlation from a theoretical model in which the fin tube surface has also been divided in two region: flooded and unflooded. The fin surface was divided into three parts (i) the fin tip and the upper corner of the fin where the condensate flow is assumed to be surface tension driven (ii) the fin flank where the condensate flows by gravity (iii) the valley part for which an empirical relation was used. Using the different heat transfer correlations for each part, they obtained the correlation:

$$Nu = Ph^{n_1} \left(\frac{D_e}{p} \right) [C_{1f} (2 - C_b) C_{ff}^{0.8} Su^{n_2} \psi^{1/2} + C_v (1 - C_b) C_{fv}^{0.8} Ga^{n_3}] + C (1 - C_b) \left(\frac{D_e b_f}{p \delta} \right) \quad (30)$$

where δ is the condensate thickness in the valley region, Su is the surface tension number, $n_1, n_2, n_3, n_4, C_r, C_v$ and C are constants which have been determined by comparison with experimental data for fluids as different as R-123, R-11, water and ethylene glycol with different fin geometries. They obtained:

$$n_1 = 0.18, n_2 = 0.25, n_3 = 0.21, n_4 = 0.51$$

$$C_r = 1.14, C_v = 2.40, C = 0.97.$$

This correlation predicts the heat transfer performance to within $\pm 30\%$ or better depending on the fluid.

A different approach was employed by Rose (1994) by using approximate relations and dimensional analysis arguments to obtain an algebraic expression of a condensation enhancement ratio ε defined as the ratio of the heat transfer coefficient of a finned tube based on the surface area of a plain tube with diameter equal to the fin root diameter, divided by that of a plain tube with diameter equal to the fin root diameter at the same vapour-side temperature difference. At given ΔT , this enhancement ratio is:

$$\begin{aligned} \varepsilon_{\Delta T} = & \frac{D_e l_f}{D_r p} T_i + \frac{\Phi (1 - f_f) (D_e^2 - D_r^2)}{\pi \cos\theta \ 2D_r p} T_f + \\ & + \frac{\Phi (1 - f_s) B_l b_r}{\pi p} T_s \end{aligned} \quad (31)$$

where

$$f_f \approx \frac{2\sigma \tan(\Phi/2)}{\rho g D_e e \Phi} \quad (32)$$

$$f_s \approx \frac{4\sigma \tan(\Phi/2)}{\rho g D_e b_r \Phi} \quad (33)$$

$$T_i = \left(\frac{D_r}{D_e} + \frac{0.51 \sigma D_r}{(\rho_l - \rho_v) g l_f^3} \right)^{1/4} \quad (34)$$

$$T_f = \left(\frac{2.82 D_r}{e_m} + \frac{0.51 \sigma D_r}{(\rho_l - \rho_v) g e^3} \right)^{1/4} \quad (35)$$

$$T_s = \left(\frac{\xi(\Phi)^3}{0.28} + \frac{0.51 \sigma D_r}{(\rho_l - \rho_v) g b_r^3} \right)^{1/4} \quad (36)$$

and e_m is a effective mean vertical fin height given by:

$$e_m = \frac{e \Phi}{\sin \Phi} \quad \text{for } \Phi \leq \pi / 2 \quad (37)$$

$$e_m = \frac{e \Phi}{(2 - \sin \Phi)} \quad \text{for } \Phi \geq \pi / 2 \quad (38)$$

and $\xi(\phi)$ a function whose a polynomial approximation is:

$$\begin{aligned} \xi(\Phi) = & 0.874 + 0.1991 \cdot 10^{-2} \Phi - 0.2642 \cdot 10^{-1} \Phi^2 \\ & + 0.5530 \cdot 10^{-3} \Phi^3 - 0.1363 \cdot 10^{-2} \Phi^4 \end{aligned} \quad (39)$$

Some of the terms of this equation depend on constants determined by fitting existing experimental data. In particular the B_1 constant is taken as $B_1 = 2.96$. Briggs and Rose (1994) improved the model by accounting for fin efficiency.

The last two methods can be easily used without iterative procedures . Moreover, the Rose method shows a correct variation of the heat transfer coefficient as a function of fin pitch.

Briggs and Rose (1999) give a detailed comparison of the results of many of the previously described models, with a large data base of experimental results.

1.3.3 Optimisation principles

Despite the considerable number of theoretical models proposed in the literature, the prediction of the optimal fin parameters (geometry, fin spacing, fin height and fin thickness) is still not accurate. As a result, interest was focused on experimental studies in order to investigate the effects of various fin parameters on the vapour-side heat transfer coefficient. In this section some investigations related to the optimal fin parameters will be presented.

a - Fin height An increase in the fin height results in a surface exchange augmentation, which enhances the heat transfer coefficient. On the other hand an increase in the fin height increases the flooded fraction and also reduces the conduction heat transfer through the fin, which deteriorates the heat transfer coefficient. These two antagonistic tendencies yield to an optimum fin height. Wanniarachchi et al. (1985) provided experimental data for steam condensation outside a horizontal copper tube with rectangularly-shaped fins. The tubes have a fin spacing of 1.5 mm, a fin thickness of 1 mm and four different fin height (0.5 mm, 1 mm, 1.5 mm and 2 mm). They found that the enhancement ratio increases with increasing fin height, but the percentage increase in the enhancement ratio is less than the percentage increase in area ratio. A fin height of 2 mm gave the best heat-transfer performance. Das et al. (1995) conducted experiments during condensation of steam on integral finned tubes. Four different material tubes (Copper, Aluminium,

Copper-Nickel and Stainless Steel) were tested, with diameters at the fin base of about 14 mm, and fin heights ranging from 0.4 to 1.5 mm. They found that when increasing the fin height the enhancement ratio increased for higher conductivity tubes (Cu, Cu-Ni and Al), and decreased with lower conductivity tubes (Stainless Steel). The Stainless Steel tube behaviour was explained by the fact that the effect of conduction through the fins is stronger for lower conductivity materials. They indicated that the optimum fin height lies beyond 1.5 mm for high conductivity tubes and may lie below 0.5 mm for Stainless Steel tube.

b - Fin thickness Wanniarachchi et al. (1985) conducted experiments on the condensation of steam on horizontal copper tubes with diameters at the fin root of 19 mm, a fin spacing of 1 mm and a fin height of 1 mm. They found a best fin thickness in the range of 0.75 mm to 1 mm. When the fin thickness was increased (> 1 mm) the surface area decreased and resulted in a decrease in the HTC. When the fin thickness was decreased below 0.75 mm, the amount of condensate retained in the interfin spaces was more important, which lead in an increased thermal resistance and a decrease in the heat transfer coefficient.

Briggs et al. (1995) experimentally investigated the fin thickness influence on the condensation heat transfer coefficient during condensation of CFC 113 and steam outside horizontal finned tubes. They tested three tubes made of different materials (copper, brass and bronze) with rectangular-section fins, having fin spacing of 1 mm, two different fin heights (0.9 mm and 1.6 mm), and fin thickness in the range 0.25 to 0.75 mm. The other geometric parameters were the same for all tubes. For CFC 113 the enhancement ratio shows a minimum for a fin thickness of 0.5 mm. This minimum was the same for all three tube materials and for both fin heights. For steam they found that there is slight increase in enhancement ratio when the fin thickness increases. They explained this by the fact that a fin thickness increase resulted in conductance of the thicker fins, which outweighs the decrease in surface area.

c - Inter-fin space The two antagonistic phenomena (the condensate drainage on the fin sides and the condensate retention) due to the surface tension forces suggests the existence of an optimal inter-fin spacing and this optimum depends on the fluid nature.

Wanniarachchi et al. (1986) experimentally studied the steam condensation on copper tubes having a diameter at the fin root of 19 mm, a fin thickness and a fin height of 1 mm. They found that the optimal inter-fin space is about 1.5 mm.

Sreepathi et al. (1996) conducted condensation experiments outside a horizontal copper tube with HCFC 123 as the working fluid. They noted that for a tube with a fin spacing of 0.85 mm and a fin thickness of 0.15 mm the optimum fin base spacing value is around 0.3 mm. They pointed out that the heat transfer performance is very sensitive to fin base spacing around the optimum value.

Belghazi (2001) condensed HFC 134a outside copper horizontal finned tubes with trapezoidal shaped fins. The diameter at the fin base is about 16 mm and the fin height is 1.4 mm. He found the optimal fin spacing to be around 0.6 mm.

d - Tube diameter An experimental study conducted by Michael et al. (1990) provides CFC 113 data during condensation on copper tubes having three different diameters (12.7 mm, 19.05 mm, and 25 mm). All the tubes have a fin thickness and a fin height of 1 mm and fin spacing of 0.25 mm, 0.5 mm, 1 mm, 1.5 mm, 2 mm and 4 mm. Although it would appear that the tube diameter has negligible effect on the heat transfer enhancement ratio due to the normalisation method, it is found that this ratio increases with tube diameter, probably due to decrease in flooding.

e - Fin shape profile The fin shape optimisation is of a great importance in the enhancement of integral-fin tube performances. Gregorig (1954) performed a theoretical study assuming that the surface tension forces are dominant, and proposed an optimal fin profile which drains more easily the condensate on the fin flanks, and gives an effective enhancement of the vapour side heat transfer coefficient.

Marto et al. (1986) conducted experiments during condensation of steam on horizontal finned tubes. Data were obtained for copper tubes with fins of rectangular, triangular, trapezoidal, and near-parabolic cross sections. They concluded that the near-parabolic fin shape providing a gradually decrease in curvature from the fin tip to the fin root results in an increase of 10 to 15 percent in steam-side heat transfer coefficient compared to the heat transfer coefficient of the three other finned tubes tested.

Webb and Murawski (1990) compared the performance of the Gewa SC tubes with a "Y" shaped fins to 1024 fin per meter integral-fin tube during condensation of R11, they found that the average condensation coefficient of the Gewa SC tube is 27 percent higher than that of the 1024-fpm tube.

Kedzierski and Webb (1990) proposed a fin profile with a curvature changing monotonically from the tip to the middle part of the fin flanks and having a small fin tip radius. A numerical study of Zhu et Honda (1993) reveals that the optimum fin shape resembles the fin shape proposed by Kedzierski and Webb (1990).

Blanc (1994) condensed R134a and R22 outside the Gewa SC and the Gewa K26 (1024 fpm) tubes. He pointed out that the vapour-side heat transfer coefficient of the Gewa K26 is 15 percent higher than the Gewa SC tube, because the retention of the condensate in the lower part of the tube is greater for the Gewa SC tube than of the Gewa K26 tube. He noted also that the Gewa SC overall heat transfer coefficient is 40% higher than the K26 value because the Gewa SC has a finned inner surface.

Honda and Makishi (1995) proposed a fin profile with a circumferential rib on the flank of a two-dimensional fin. They concluded that the circumferential ribbing enhances the film condensation on a horizontal two-dimensional fin tube. The enhancement is more significant for a double rib than for a single rib fin.

1.4 Low integral finned tube bundle

The models developed for a single enhanced tube are not directly applicable to tube banks, since the heat transfer in the lower rows is affected by condensate inundation and the HTC is lower for these tubes. In the literature there are two approaches to this problem:

The first simply consists in applying the Nusselt approach developed initially for smooth tubes. Katz & Geist (1948) proposed a correlation in the form of equation (15) with g equal to 0.04 instead of $1/4$ as proposed by Nusselt in the smooth tube bundles. The second consists in developing a model, first for a single tube, and then for a bundle, by considering two different situations according to whether the lower tubes are unflooded or flooded by the condensate flowing from the upper tubes. Such a model was proposed by Honda et al. (1989) who extended their model developed initially for a single horizontal finned tube. In this model they calculate separately the heat flux in the flooded and unflooded regions for the top tube row. For the second and subsequent rows they distinguish the flow mode of impinging condensate using the following criteria:

Column mode for $K \leq 0.42$

Sheet mode $K > 0.42$

with

$$K = \frac{\Gamma}{2} (g / \rho_l)^{1/4} / \sigma^{3/4} \quad (40)$$

where Γ is the flow rate of falling condensate per unit length.

In the column mode case there is an affected (A-region) and an unaffected (U-region) regions, whereas in the sheet mode case there is just one region (A-region) see figure (6). Then, they calculate the heat flux for each region and deduce the average heat flux of the considered tube as in the single tube case, taking into account the proportion of surface area covered with impinging condensate.

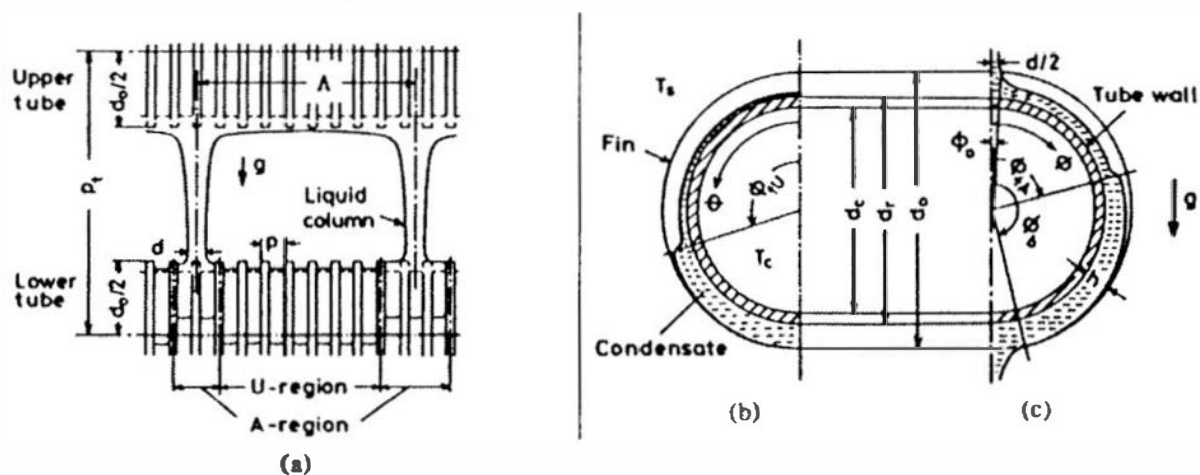


FIGURE 6. Physical model of Honda et al. (1989).

The comparison of this model to the experimental results of Marto (1986) who provided data of steam condensation outside a bundle of horizontal finned tubes shows an under-estimation of experimental results ranging from 5% to 20%.

Murata & Hashizume (1992) developed a model predicting the HTC of tube bundles having rectangular fins. For this purpose they carried out an analysis of the film condensate. The inundation is taken into account through the condensate flow rate of the upper tubes which leads to a modification of the condensate thickness in the interfin space. To validate their model they compared it to experimental data during condensation of R11 and R114 in bundles of 8 rows, with rectangular fin tubes of various fin pitches. Theory and experiments differed by about 20%. Belghazi (2001) provided data of HFC 134a condensation outside five commercial horizontal finned tubes (K11, K19, K26, K32 and K40 tubes having 11, 19, 26, 32 and 40 fins per inch respectively). He found that the Katz & Geist (1948) correlation gives good results for the tubes having high fin densities (K26, K32 and K40) but underestimates the inundation effect for the K11 and K19 (Figure 7).

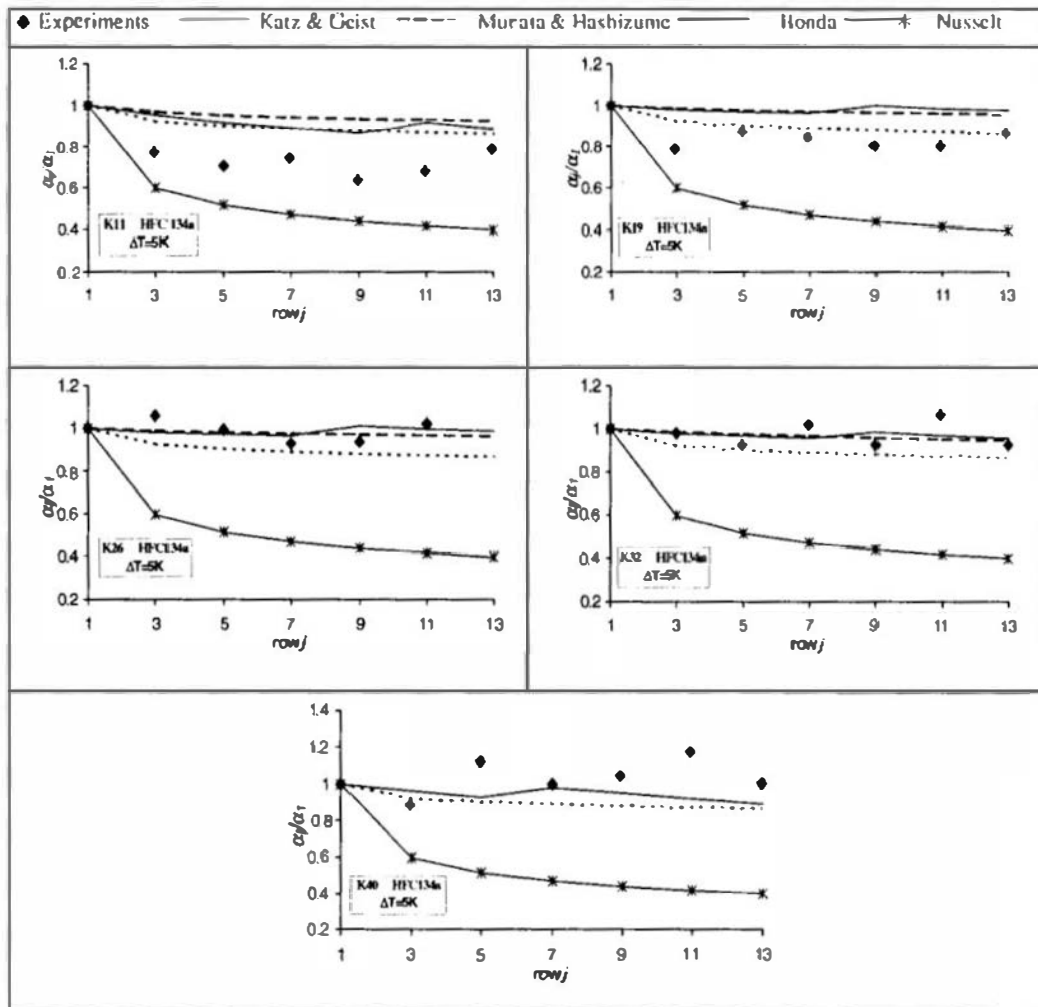


FIGURE 7. Heat transfer coefficient in a tube bundle during condensation of HFC 134a (Belghazi, 2001).

He also pointed out that the Honda et al. (1989) and Murata & Hashizume (1992) models did not give a significant amelioration in comparison to the Katz & Geist (1948) correlation (Figure 7), despite of their rather complex approaches.

1.5 Special enhanced surface tubes (3D)

1.5.1 Single tube

A lot of geometries have already been tested, for example, spines (Webb et al., 1982), saw-tooth shape (Webb and Murawski, 1990, Cheng and Tao, 1994), Gewa C+ (Belghazi, 2001).

Such 3-D geometries should enhance the surface tension drainage. However, to our knowledge, few authors developed arguments to justify the fin shape except Webb et al. (1982) for spine-fins tubes and Belghazi (2001) for the Gewa C+ tube.

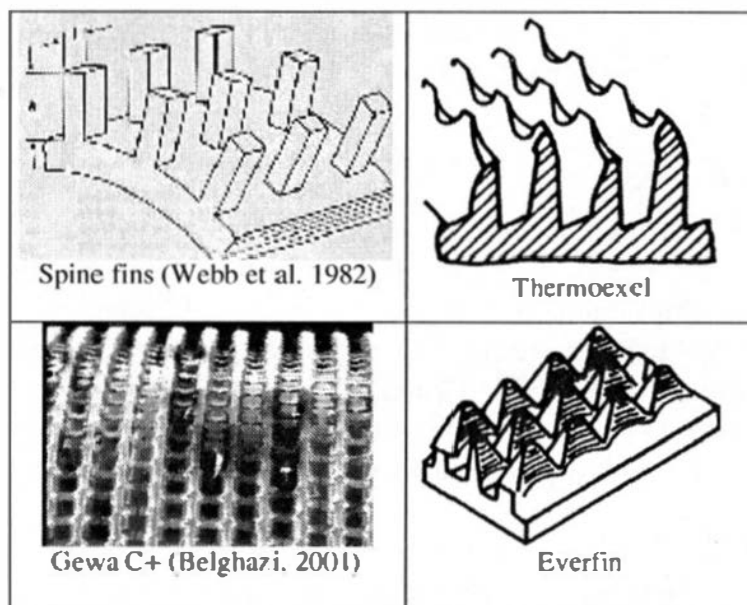


FIGURE 8. Three-dimensional tube geometries.

To study the surface tension effects in 3-D geometries (spines), experiments were conducted by Webb et al. (1982). A gravity based model failed to represent experimental results whilst a surface tension based model predicted the condensation coefficient within 10%.

Belghazi (2001) developed a model to determine the heat transfer coefficient during condensation of HFC 134a on a Gewa C+ tube (Figure 8). He divided the tube into four regions : (a) the fin region upon the notch, (b) the fin region below the notch, (c) the fin flank between two notches and finally the circumferential region between the fins. He assumed that the condensate flow is surface tension driven in the regions (a) and (c), and is gravity driven in the regions (b) and (d). The heat transfer coefficient is given by : α_b and α_d are calculated from the Nusselt correlation for a vertical plane plate and for a

$$\alpha_e = \eta_f (\alpha_a A_a + \alpha_b A_b + \alpha_c A_c) + \alpha_d A_d \quad (41)$$

smooth horizontal tube respectively. α_a and α_c are also calculated from the Nusselt expression for a vertical plane plate, where the gravity force $\rho_l g$ is replaced by an equivalent in terms of surface tension. He found that this model agrees fairly ($\pm 10\%$) with the experimental results.

1.5.2 Tube bundle

Webb & Murawski (1990) presented experimental results of condensation of R11 on the shell side of a vertical bank of five horizontal tubes. They compared two kinds of three-dimensional tubes (Turbo C and Tred D) to integral fin tubes (1024 fpm) and to the Gewa SC tubes. They pointed out that the turbo C tube shows the highest single-tube performance.

They found that the data for all tubes follow similar curves, when plotted in α_j versus Re the condensate Reynolds number, the straight line curve fits yield equations of the form:

$$\alpha_j = C Re^{-\omega} \quad (42)$$

They found further that ω is equal to 0.58, 0.51, 0.22 and almost zero for the Tred D, Turbo C, Gewa SC and the integral-fin tube respectively concluding that the Turbo C and the Tred D have an important inundation effect.

Cheng & Wang (1994) tested three three-dimensional tubes and compare its performances to low integral finned tubes of 26, 32 and 41 fins per inch, during condensation of stationary vapour of HFC 134a on a bundle of three rows. They concluded that the row effect (inundation effect) is more pronounced for three-dimensional-fin tubes than for low-fin tubes.

Honda et al. (1991)(1992) conducted experiments during condensation of R113 on staggered and on in-line bundles of three-dimensional tubes and of flat-sided-fin tubes. They found that the inundation is more important in the in-line bundle than in the staggered bundle, and there is more inundation in the case of three-dimensional-fin tube bundle compared to the flat-sided-fin tube bundle. The same conclusion was found by Belghazi (2001) for condensation of HFC 134a.

2. VAPOUR MIXTURE

2.1 General

The studies of condensation heat transfer of mixtures were first linked to petrochemical problems and the first theories of mixture condensation were established 65 years ago with the work of Colburn and Hougen (1934). Their interest has increased again during

the last decade with the use of new refrigerant mixtures. Nevertheless, there are very few publications on condensation heat transfer of mixtures on horizontal smooth or finned tubes. We can only cite two previous review papers: the first from Wang and Chato (1994) and the second from Thome (1994). An interesting review on condensation of mixtures on flat and finned vertical plates must be cited (Hijikata and Himemo, 1990) because the main parameters controlling heat and mass transfer are discussed. A list of recent theoretical studies of steady laminar film condensation of a multicomponent vapour mixture on a flat plate is given by Rose et al. (1999). In this section we will give an overview of current theories and of the experimental results with underlining the main features compared to pure fluid condensation. Some new results obtained with the R23/R134a mixture will serve as a base of discussion.

2.2 Current theories

For a mixture of several vapours, two cases have to be considered. First, when the mixture forms an azeotrope, the behaviour of the fluid is similar to that of a pure fluid.

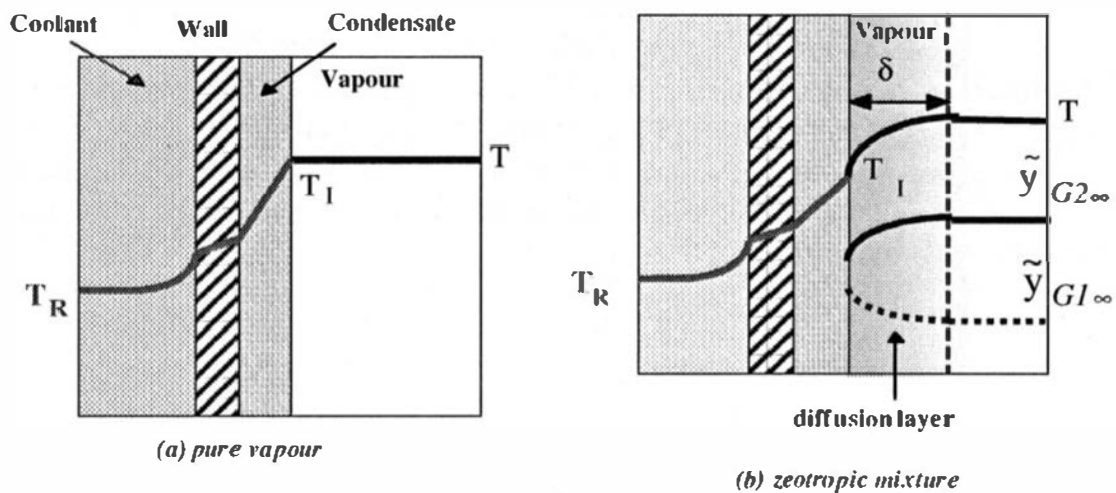


FIGURE 9. Temperature profiles near the wall: (a) Pure fluid or azeotrope. (b) Zeotropic mixture.

In this case, the temperature profile near the wall is comparable to the one seen figure 9 (a). On the contrary, for a zeotropic mixture, the less volatile vapour condenses preferentially, the more volatile accumulating near the liquid-vapour interface thus creating a layer (called diffusion layer) through which the less volatile component must diffuse (Figure 9 (b)).

As shown in figure 9 (a), the main resistance to heat transfer is located in the condensate film for condensation of a pure fluid. For a zeotropic mixture an additional thermal resistance due to the vapour diffusion layer affects heat and mass transfer towards the interface. In most cases this latter resistance controls the condensation process. To determine the heat and mass flow rates, two methods are currently in use:

- an equilibrium method called the “condensation curve” or “cooling curve” theory,
- the film method.

Others methods have been developed which consist to solve the boundary layer equations for natural or forced convection of the vapour mixture parallel to a flat plate or perpendicular to a smooth tube.

2.2.1. Condensation curve methods In these methods, developed by Silver (1947) and Bell and Ghaly (1973), the fluids (vapour, gas and condensate) are assumed to be locally in equilibrium throughout the condenser. In the Silver method the heat transfer coefficient α_{ext} between the bulk gas and the condenser wall is calculated by:

$$\frac{1}{\alpha_{ext} A_0} = \frac{1}{\alpha_l A_l} + \frac{Z_g}{\alpha_g A_l} \quad (43)$$

In this equation, α_l is the heat transfer coefficient for the condensate layer and the heat transfer coefficient α_g is calculated for the gas phase flowing along the condenser by itself. A_0 and A_l are respectively the reference surface area and the actual external surface area of a tube, A_0 being equal to A_l for smooth tubes. The α_g coefficient can be corrected for mass transfer effects by writing (McNaught, 1979)

$$\alpha_g^* = \alpha_g \frac{\psi}{e^{\psi} - 1} \quad (44)$$

where

$$\psi = \frac{\dot{n}_T \tilde{c}_{p,g}}{\alpha_g} \quad (45)$$

\dot{n}_T being the molar flux of the condensing vapour.

The Z_g coefficient is given by

$$Z_g = X_g \tilde{c}_{p,g} \frac{dT}{dh_m} \quad (46)$$

where X_g is the mass flow fraction of the gas, $\tilde{c}_{p,g}$ is the specific heat of the gaseous mixture and dT/dh_m is the inverse slope of the equilibrium condensation curve $h_m = f(T)$, h_m being the specific enthalpy of the fluid. Typical condensation curve for a binary mixture

is given in figure 10. In the liquid-vapour zone, one can distinguish 3 types of curves: (a) the concentration of the more volatile component is greater than that of the less volatile, (b) the two components have nearly the same concentration, (c) the concentration of the more volatile component is smaller than that of the less volatile.

The main interest of this method is its simplicity, since the mass transfer parameters need not be known (diffusion coefficients in particular). It is sufficient to determine the condensation curve and the heat transfer coefficients α_l and α_g^* .

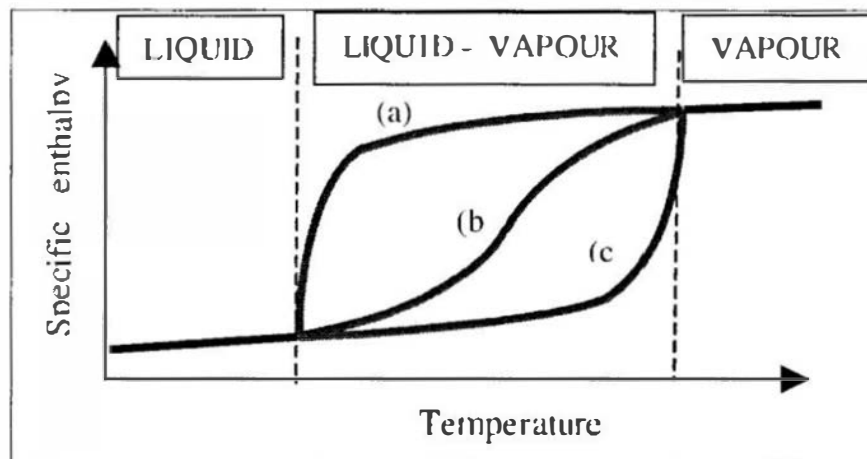


FIGURE 10. Specific enthalpy of a binary mixture as a function of temperature for different concentrations of the components.

If \dot{Q} is the heat flow rate, the local overall heat transfer coefficient U between the gas and the coolant is defined by:

$$\dot{Q} = U A_0 (T_g - T_c) \quad (47)$$

where T_g is the bulk gas temperature, T_c the coolant temperature and where U is calculated by adding the thermal resistances:

$$\frac{1}{U A_0} = \frac{1}{\alpha_{cool} A_i} + r_{wall} + \frac{1}{\alpha_{ext} A_f} \quad (48)$$

where α_{cool} is the coolant side coefficient, A_i the internal heat exchange surface area and r_{wall} the thermal resistance of the tube wall.

2.2.2 Film theory This theory was first developed by Colburn and Hougen (1934) for condensation of a vapour in the presence of a non-condensable gas and extended by Colburn and Drew (1937) to condensation of a zeotropic binary mixture. Then, it was improved by Ackermann (1937). The heat transfer coefficient $\alpha_{c,l}$ between the condensate/gas interface and the coolant is defined by the heat balance equation:

$$\alpha_{cl} (T_l - T_c) = \alpha'_g (T_g - T_l) + \Delta h_{lv} \beta_D^* \frac{\tilde{Y}_v - \tilde{Y}_l}{1 - \tilde{Y}_v} \quad (49)$$

where T_l is the interface temperature, Δh_{lv} the molar latent heat of condensation, \tilde{Y}_v and \tilde{Y}_l are the mole fraction of the vapour in the bulk gas and at the interface respectively. β_D^* is the corrected mass transfer coefficient given by:

$$\beta_D^* = \beta_D \frac{\Xi}{e^\Xi - 1} \quad (50)$$

where

$$\Xi = \frac{\dot{n}_T}{\beta_D} \quad (51)$$

\dot{n}_T is the total molar condensed flow rate and β_D is the mass transfer coefficient which can be obtained from the analogy between heat and mass transfer (Chilton and Colburn, 1934):

$$\beta_D = \frac{\alpha_g}{\tilde{c}_{pg}} \left(\frac{Pr}{Sc} \right)^{2/3} \quad (52)$$

This coefficient can be calculated by using standard correlations for α_g or by adapting these correlations from specific experiments (Honda et al., 1999).

On the other hand, the α_{cl} coefficient is given by:

$$\frac{1}{\alpha_{cl} A_0} = \frac{1}{\alpha_{cool} A_i} + r_w + \frac{1}{\alpha_l A_l} \quad (53)$$

The heat transfer coefficient α'_g is the gas-phase coefficient corrected for mass transfer effect as:

$$\alpha'_g = \alpha_g \frac{\Psi}{1 - e^{-\Psi}} \quad (54)$$

The local overall heat transfer coefficient may be defined as:

$$\dot{Q} = U A_0 (T_g - T_c) = \alpha_{cl} A_0 (T_l - T_c) \quad (55)$$

A systematic comparison between the film and the condensation curve methods was conducted by Webb et al. (1996) who indicated the limits of the latter method.

2.3 Smooth tubes

2.3.1 Single horizontal smooth tube Many papers have been published on condensation on horizontal smooth tubes, in the presence of non-condensing gas. To the authors' knowledge, few studies have been carried out on condensation of a vapour mixture on a smooth

tube and most of them up to 1990) were listed by Fuji et al. (1990). The first theoretical study seems to be the one by Denny and South (1972). These authors developed the boundary layer equations to investigate the effect of binary mixture condensation at the forward stagnation point of a horizontal cylinder and gave numerical results for a steam-methanol mixture. Kuang and Chen (1985) adapted the Nusselt equation to the case of a zeotropic mixture by replacing the leading constant 0.728 and the exponent 1/4 by two constants A0 and A1 respectively. These constants were fitted with the experimental results for 4 mixtures: R11/R12, R11/R22, R11/R502, and R11/R12/R22. Fujii et al. (1990) studied several different patterns of gravity-controlled condensation of binary mixtures on a single smooth horizontal tube, and Hijikata and Himeno (1990) studied the performances of the binary mixture CFC113/CFC114 on a smooth tube while including the influence of the vapour flow direction on the heat transfer performance. Wang et al. (1995) solved the boundary layer equations in the case of natural convection neglecting the pressure gradient in each phase and compared their model to the results of the experiments carried out with the binary mixture HFC152a/HCFC22 (Figure 11). The complete equation system for condensation of a binary mixture on a smooth horizontal tube has been given by Belghazi (2001). Signe et al. (1998) and Belghazi et al. (2001) presented experimental results for the R23/R134a zeotropic mixture. The experimental results of these two latter authors are summarised in figure 12 where the heat transfer coefficients as a function of $\Delta T = T_b - T_w$ (T_b is the bulk vapour temperature and T_w the tube wall temperature), are represented.

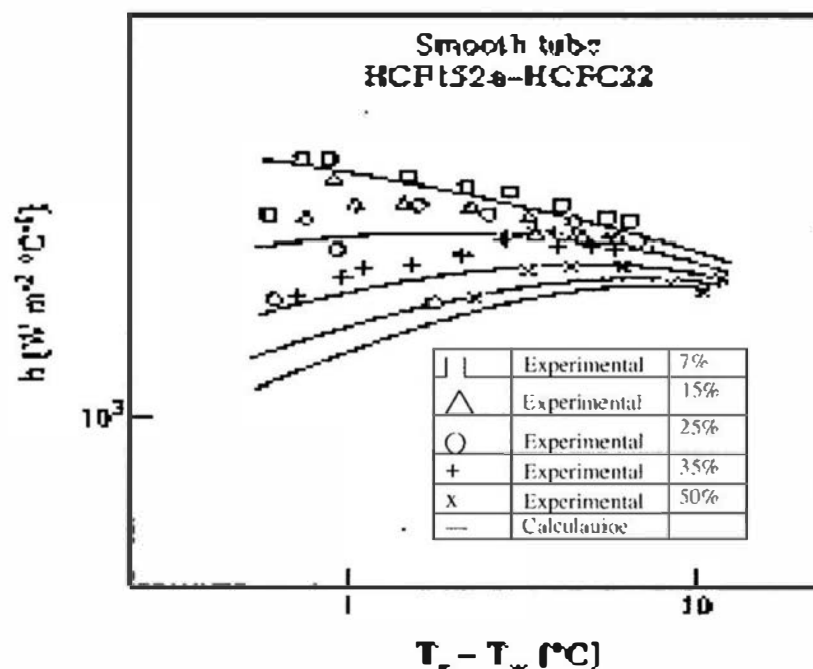


FIGURE 11. Condensation heat transfer coefficient as a function of ΔT for the R152a/R22 mixture at different concentrations (After Wang et al., 1995).

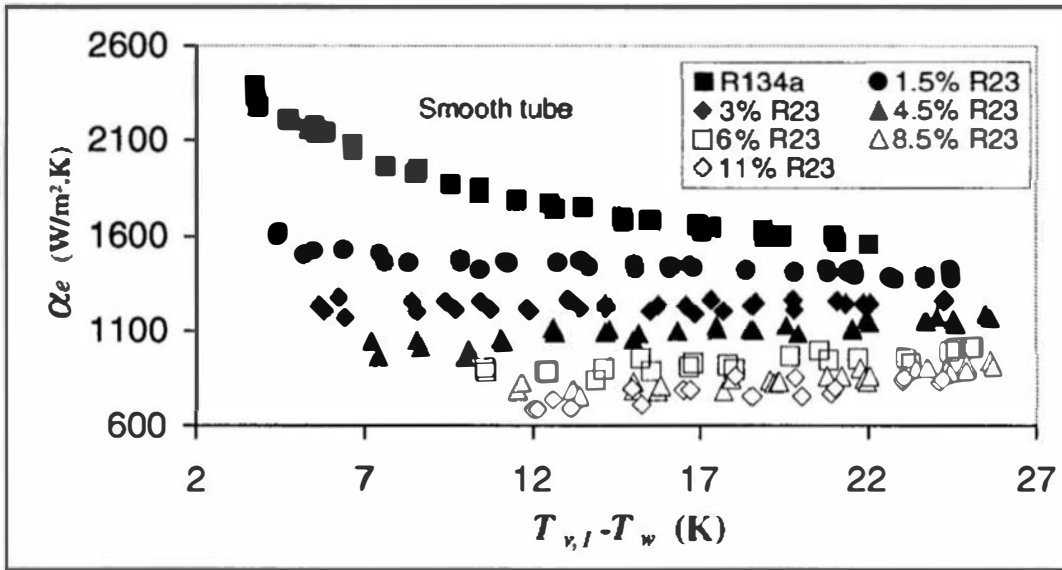


FIGURE 12. Condensation heat transfer coefficient as a function of ΔT for the R23/R134a mixture at different concentrations.

These results can be analysed similarly to those of Hijikata et al. (1990) for a flat plate:

- (i) The results tend to the Nusselt solution as ΔT increases.
- (ii) In the small ΔT region the heat transfer coefficient is rate controlled by the diffusion layer
- (iii) The value of the heat transfer coefficient could be explained by considering that the thermal resistances of the liquid film and of the diffusion layer coexist independently in series.

The use of the condensation curve theory allows these results to be qualitatively interpreted. In the small ΔT region the α_l value is very high (Nusselt theory) and the corresponding thermal resistance is low. Moreover, in the case of the lowest concentrations of the more volatile component, the corresponding condensation curve is the (c) curve in figure 10. In this case, the slope of the condensation curve dh/dT at the dew point T_d is high leading to a small value of the Z/α_g factor i-e to a high value of the corresponding thermal resistance. Conversely, for higher concentrations, the slope of the condensation curve at T_d is low and it can be written:

$$\left. \frac{Z_g}{\alpha_g} \right|_{R23 \text{ low concentration}} < \left. \frac{Z_g}{\alpha_g} \right|_{R23 \text{ high concentration}} \quad (56)$$

In accordance with the experimental results, for a given ΔT , the condensation heat transfer coefficient for low concentration or the more volatile component (R23) is higher than that for high concentration. For high ΔT value, the heat transfer is rate controlled by the condensate film because the reverse mass diffusion becomes negligible.

The theoretical analysis of these results has been made with the condensation curve method (Figure 13). If the agreement is fairly good for the very small concentration in the more volatile component (1.5 % in R23), it is rapidly becoming worse as this concentration increases. The authors proposed, as suggested by Webb et al. (1996), to introduce the Lewis number Le in the formula (43):

$$\frac{1}{\alpha_{ext} A_0} = \frac{1}{\alpha_l A_l} + \frac{Le^{3/2} Z_g}{\alpha_g A_l} \quad (57)$$

with

$$Le = \alpha / \mathcal{D} \quad (58)$$

α being the thermal diffusivity and \mathcal{D} the mass diffusivity of the mixture. In this case the agreement is rather good, even for high concentrations of the more volatile component.

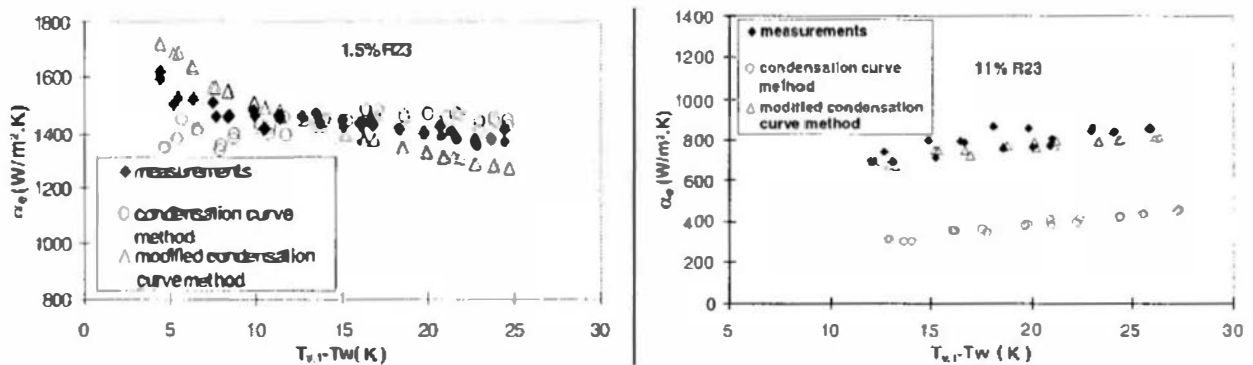


FIGURE 13. Condensation of R23/R134a mixture: Comparison of experimental results with classical and modified condensation curve theories.

2.3.2 Smooth tube bundle A crucial problem in the heat transfer coefficient measurements in condensation of a vapour mixture in a bundle of tubes is the choice of the vapour temperature. Indeed, the bulk vapour temperature is strongly dependent on the position in the condenser. Moreover, condensation can occur on the temperature sensor itself leading to an erroneous measurement. A way of avoiding such problems is to use only one temperature, the dew temperature being generally chosen. Several authors on the contrary have placed thermocouples inside the bundle either by shielding the thermocouple under a dummy tube (Signe et al., 1998, Belghazi et al., 2001) to measure the vapour temperature

or by attaching a shield and a gutter just above and below the thermocouple to measure the vapour and the condensate temperature respectively (Honda et al., 1999). An example is shown on the figure 14 in which the local vapour temperature is measured for a given composition of the mixture R23/R134a (Belghazi et al., 2001). Contrary to pure fluids, no influence of the inundation effect on the heat transfer coefficient was observed. It can be noticed that theoretical calculations using the modified condensation curve method are in good agreement with the experimental results.

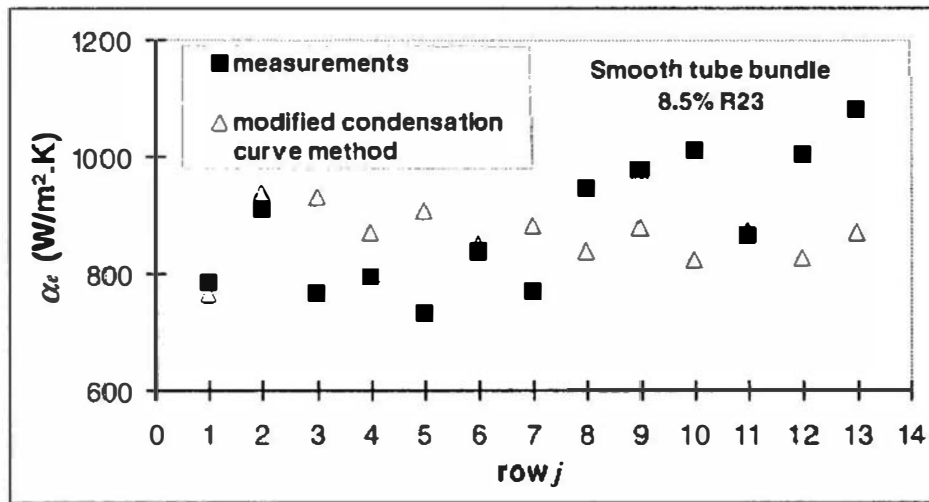


FIGURE 14. Condensation of R23/R134a mixture: Heat transfer coefficient as a function of the row number. Comparison between experimental results and modified condensation curve theory.

2.4 Finned tubes

2.4.1 *Single horizontal finned tubes* A resumé of results for the condensation of zeotropic mixtures on the outside of finned tubes is shown in table 1.

Reference	Fluid	T _v (°C)	Tested surface
Hijkata et al. (1986)	R113/R11		Finned tube
Murphy, Chen and Hwang (1988)	R12/R114	40.5	Low finned tubes (Single tube)
Hijkata, Himeno and Goto (1990)	R113/R114	Various	Smooth and low finned tubes (Single tube)
Sami and Schnotale (1992)	R22/R114 R22/R152a		Low finned tube (Single tube)
Belghazi, Signe, Bontemps and Marvillet (1998)	R23/R134a	40°C	Low finned tubes (Single tube and tube bundle)
Honda, Takamatsu and Takata (1999)	R123/R134a	50 °C	Low finned tube (Tube bundle)

TABLE 1. Condensation studies on finned tubes with vapour mixtures.

From the experimental studies of Murphy et al. (1988), Hijikata et al. (1990) and Belghazi et al. (1998), the first general conclusion is that the higher concentration in the more volatile component and the more degraded the heat transfer coefficient if compared to the less volatile component one. This can be observed in figure 15 from the Hijikata and Himeno studies (1990) for condensation of R113/R11 and R113/R114 and in figure 16 which corresponds to a complete study carried out for condensation of a R23/R134a mixture on low finned tubes whose fin pitches varied from 11 to 40 fpi.

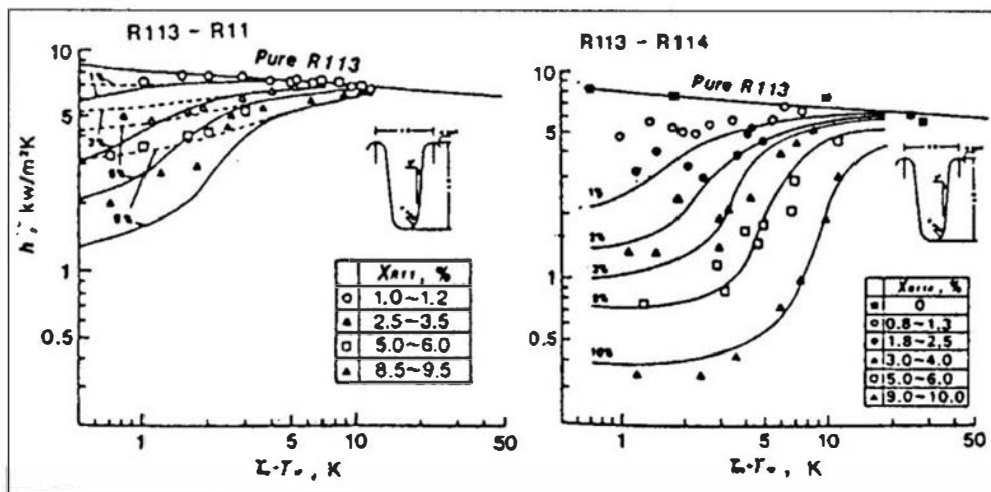


FIGURE 15. Heat transfer coefficient of free convective condensation of mixtures on a high-fin tube (after Hijikata et al., 1986).

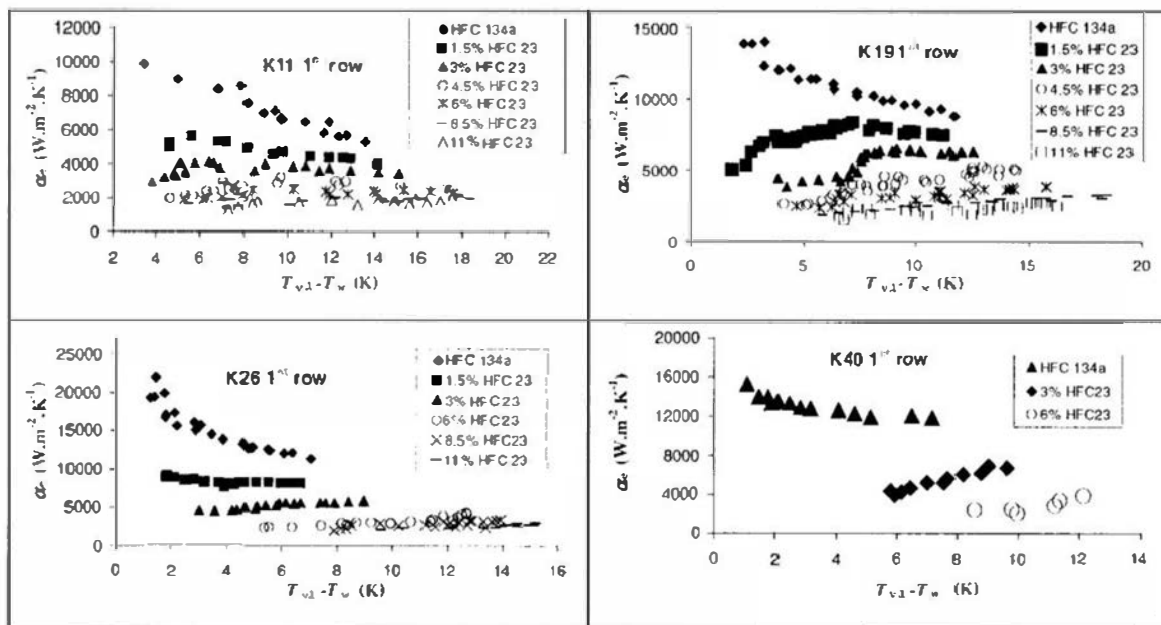


FIGURE 16. Condensation heat transfer coefficient for R23/R134a mixtures with different composition on finned tubes.

The following remarks, some being similar to those for a smooth tube, can be done:

- (1) A small amount of the more volatile component is sufficient to create a diffusion barrier which controls the heat transfer and causes the heat transfer coefficient to be strongly decreased.
- (2) As for a smooth tube, in the small ΔT region the heat transfer coefficient is rate controlled by the diffusion layer
- (3) As ΔT increases, the heat transfer coefficient for a finned tube increases markedly, while it increases only slightly for a smooth tube.
- (4) At high ΔT the heat transfer coefficient tends towards the heat transfer coefficient of the less volatile fluid.
- (5) The more important the mass fraction of the more volatile component, the greater the decrease in the heat transfer coefficient.
- (6) At high concentration of the more volatile fluid the heat transfer coefficient tends to an asymptotic limit.
- (7) When the concentration of the more volatile component has a significant value ($> 3\%$ in this case), the order of magnitude of the heat transfer coefficient is barely dependent on the concentration.

To the above, one can add the results of Hijikata and Himeno (1990) who remark that contrary to the pure fluid case, the best performances are obtained with high fins when a vapour mixture is condensing. Considering the figure 17, it can be seen that the thickness of the diffusion layer greater or smaller than the fin height. If the thickness is small compared to the fin height, the wavy heat exchange surface area is greater than the projected area of the tube. Conversely, for a thickness greater than the fin height, the heat exchange surface area is approximately the same as the projected area and the heat transfer coefficient diminishes. For small ΔT , the fins are covered by the diffusion layer and the heat transfer coefficient strongly decreases. As the condensate film thickness increases, the temperature difference between the vapour bulk and the liquid-vapour interface decreases and the diffusion layer is thinned. The fins are no longer covered by the diffusion layer leading to a significant augmentation of the heat transfer coefficient.

As for smooth tubes, a theoretical analysis can be carried out by the condensation curve method. In the case of finned tube the formula (57) has been adapted by the simple following way: the orders of magnitude of the heat transfer coefficients α_l and α_g are very different (factor 100 to 200). The choice of an accurate theory to determine α_l is less important than in the case of pure fluids. It is the reason why in this case the Beatty and Katz formula was chosen. On the other hand, the gas heat transfer is efficient on the unflooded part of fins, and the formula (57) becomes:

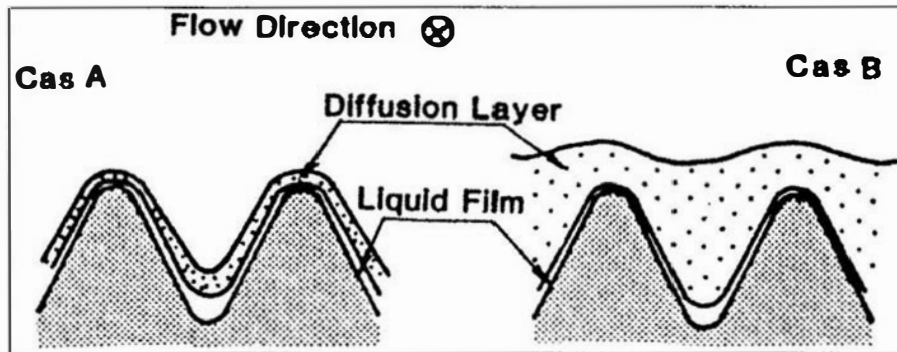


FIGURE 17. Comparison between diffusion layer thickness and fin height (After Hijikata and Himeno, 1990).

$$\frac{l}{\alpha_{ext} A_f} = \frac{l}{\alpha_l A_l} + \frac{Le^{3/2} Z_g}{\frac{\Phi}{\pi} \alpha_g A_l} \quad (59)$$

It can be seen in the figure 18 that the agreement is fairly good for low concentrations in the more volatile component but this agreement becomes poorer as the concentration increases.

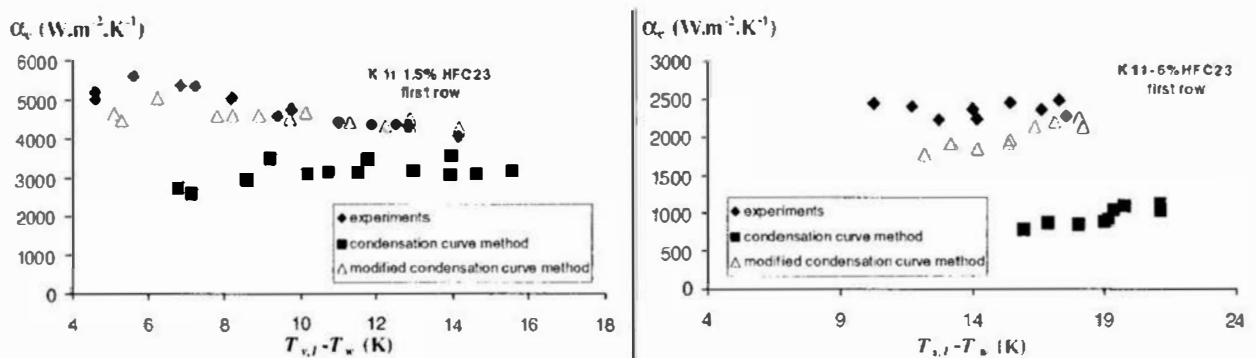


FIGURE 18. Condensation of R23 /R 134a mixture. Comparison of experimental results with condensation curve theory.

This poor agreement can be explained by remarking that the dependence with the Lewis number is not as simple as it is proposed in the formula (59).

2.4.2. *Finned tube bundle* It has been seen that, for pure fluids, the inundation of lower tubes in a bundle has a smaller effect for finned tubes than for smooth tubes. In the case of a mixture, the bulk vapour temperature varying strongly between the condenser inlet and the outlet, this tends to increase the value of the heat transfer coefficient. The combination of these two effects can make the heat transfer coefficient be increased compared to the first row of the bundle. This is observed in figure 19 for the condensation of R23/R134a on tubes with 19 fpi.

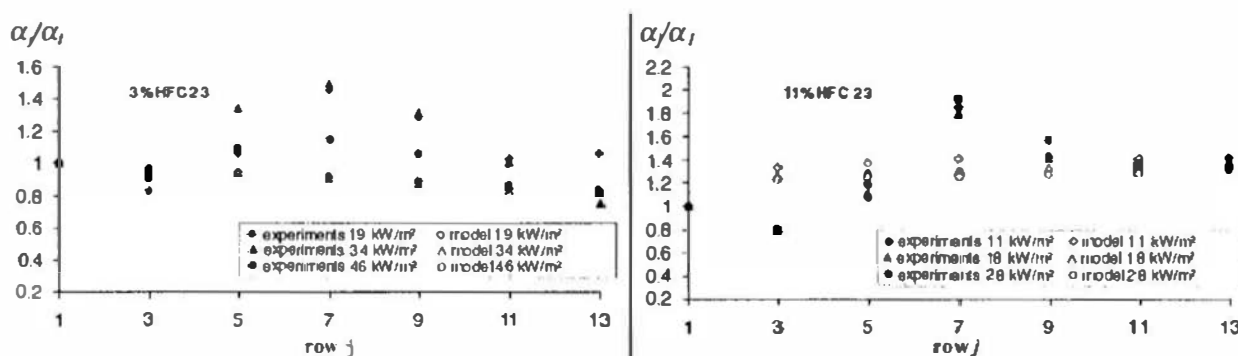


FIGURE 19. Condensation of R23/R134a mixtures on finned tubes with 19 fins per inch. Ratio of the heat transfer coefficient of the j th row by the heat transfer coefficient of the first row as a function of the row number.

In this figure, together with experimental results are given the theoretical interpretation with the modified condensation curve model. The strong variations of the heat transfer coefficient cannot be represented by this method. However, the total heat power is calculated with a good accuracy ($\pm 10\%$, Figure 20)

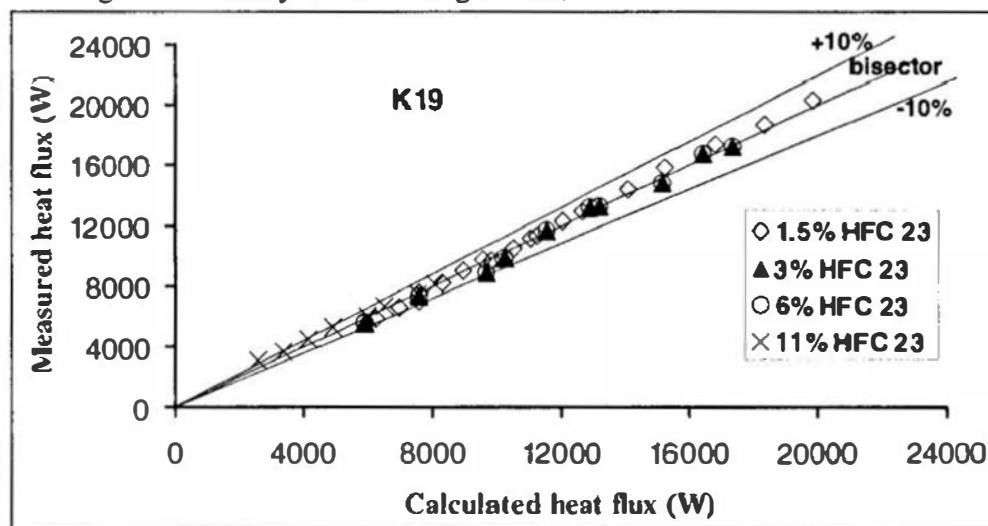


FIGURE 20. Measured heat flux as a function of the heat flux calculated with the condensation curve method.

2.5 Enhanced surface tubes

The condensation of a vapour mixture on enhanced surface tubes has induced less studies than for pure fluids. Indeed, the first industrial approach is to use the tubes manufactured for pure fluids. As an example, the heat transfer coefficient for condensation of the R23/R134a mixture Gewa C+ tube is given in figure 21. It can be observed a drastic fall of the heat transfer coefficient even at low concentration of R23.

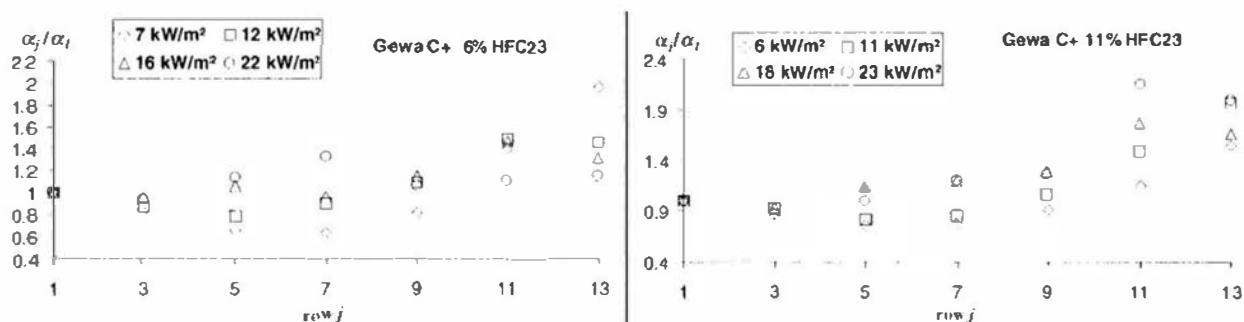


FIGURE 21. Condensation of R23/R134a mixtures on Gewa C+ tubes. Ratio of the heat transfer coefficient of the j th row by the heat transfer coefficient of the first row as a function of the row number.

In this particular case, this can be explained by remarking that the fin height of this tube is slightly smaller than that of the trapezoidal fins previously studied. The fins are completely covered by the diffusion layer.

CONCLUSION

The effects of the different parameters (tube geometries and fluid properties) on shell-side condensation heat transfer are presented in this paper. Low-finned tubes (2D geometries) are currently in use in shell-and-tube condensers and special enhanced surfaces (3D geometries) are in development. These two types of tubes are used with pure fluids as well as with vapour mixtures. The main conclusions that can be drawn are:

Low finned tubes. Single tube. Pure fluid.

- (i) The heat transfer enhancement factor compared to a smooth tube can vary from 5 to 10.
- (ii) The optimal configuration of fins is close to being established. The presence of ribs on the fin flanks add a supplementary enhancement factor.
- (iii) The retention of the condensate on the underside of the tubes has a detrimental effect on heat transfer. More research is needed to minimise this effect.

- (vi) The models of Honda et al. (1987) and Rose (1994), allow the heat transfer coefficient to be predicted with a good accuracy. However, the Rose model is more easy to use.

Low finned tubes. Tube bundle. Pure fluid.

- (i) Low-finned tubes are barely affected by the inundation effect.
- (ii) The problem of the tube arrangement in a shell-and-tube heat exchanger is not completely solved.
- (iii) The model of Honda et al. (1987) is the most complete which predicts the heat transfer coefficient of a bundle. However, the inundation effect can be predicted with a correlation of Nusselt type having an exponent varying from 0 to 0.07.

Special enhanced surface tubes. Single tube. Pure fluid.

- (i) 3D surfaces have been shown to have heat transfer coefficients greater than 2D surfaces.
- (ii) No general models exist. Specific geometries have specific models.

Special enhanced surface tubes. Tube bundle. Pure fluid.

- (i) 3D surfaces can be strongly affected by the inundation effect.

Low finned and enhanced surface tubes. Vapour mixtures.

- (i) A small amount of the more volatile component produces a strong decrease in the heat transfer coefficient compared to that of the pure less volatile fluid.
- (ii) The classical condensation curve method underestimates the experimental results. This method was adapted by introducing the Lewis number. Theoretical results are in good agreement with experimental results especially for low concentrations of the more volatile component.
- (iii) The 3D surfaces are not any more efficient than 2D surfaces since the thermal resistance of the diffusion layer controls the heat transfer.

NOMENCLATURE

		<i>Latin letters</i>
a	$\text{m}^2.\text{s}^{-1}$	Thermal diffusivity
A	m^2	Heat transfer surface area
b_r	m	Fin spacing at fin root

b_f	m	Fin spacing at fin tip
c_i		Constants in the Sreepathi correlation ($i = 1 - 4$)
C_b		Flooded region fraction
c_p	J. kg ⁻¹ .K ⁻¹	Specific heat capacity (massic)
\tilde{c}_p	J. mol ⁻¹ .K ⁻¹	Specific heat capacity (molar)
\tilde{D}	m	Diameter
\mathcal{D}	m ² .s ⁻¹	Mass diffusivity
e	m	Fin height
g	m.s ⁻²	Gravity
j		Row index
L	m	Length
\dot{m}	kg.s ⁻¹	Mass flow rate
n		Row number
$\dot{\tilde{n}}$	mol.s ⁻¹	Molar flow rate
N_f		Number of fins per metre
p_f	m	Fin pitch
\dot{Q}	W	Heat flow rate
t_r	m	Fin thickness at fin root
t_t	m	Fin thickness at fin tip
T	K	Temperature
U	W.m ⁻² .K ⁻¹	Overall heat transfer coefficient
X_g		Vapour mass fraction
\bar{Y}		Mole fraction
Z_g		defined in equation (46)

Greek letters

α	W.m ⁻² .K ⁻¹	Heat transfer coefficient
$\bar{\alpha}$	W.m ⁻² .K ⁻¹	Average heat transfer coefficient
β	mol.m ⁻² .s ⁻¹	Mass transfer coefficient
δ	m	Diffusion layer thickness
Δh_w	J.kg ⁻¹	Latent heat
ϵ		Enhancement ratio
γ		inundation coefficient
Γ	kg. m ⁻¹ . s ⁻¹	Lineic mass flow rate
η		Fin efficiency
λ	W.m ⁻¹ .K ⁻¹	Thermal conductivity
μ	Pa.s	Dynamic viscosity

ω		Inundation coefficient
ρ	kg. m ⁻³	Density
σ	N. m	Surface tension
θ	Rad	Fin angle
ψ		$(\dot{m} \bar{c}_{p,g}) / \alpha_g$
Φ	Rad	Angle of unflooded part
Φ_f	Rad	Angle of flooded part
ξ		Function in formula (39)
Ξ		\dot{m}_T / β_D

Subscripts

<i>cl</i>	cooling fluid/interface
<i>cool</i>	cooling fluid
<i>eq</i>	equivalent
<i>ext</i>	external
<i>f</i>	fin, fin flank
<i>g</i>	gas
<i>i</i>	internal
<i>l</i>	interface
<i>l</i>	liquid
<i>m</i>	mixture
<i>sat</i>	saturation
<i>t</i>	total
<i>v</i>	vapour
<i>w</i>	wall

Dimensionless numbers

<i>Ga</i>	Galileo number
<i>Nu</i>	Nusselt number
<i>Nu*</i>	Condensation Nusselt number
<i>Ph</i>	Phase change number
<i>Pr</i>	Prandtl number
<i>Re</i>	Reynolds number
<i>Su</i>	Surface tension number

REFERENCES

- Ackermann, G. 1937. Wärmetübergang und molekulare Stoffübertragung im gleichen Feld bei grossen Temperatur und Partialdruckdifferenzen. (Simultaneous heat and mass transfer with large temperature and partial pressure differences). *V.D.I. Forschungshft.* 382 (8): 1-16, (in German)
- Adamek, T. 1981. Bestimmung der Kondensations-grossen auf Feigewellten Oberflächen zur Auslegung Optimaler Wandprofile. *Wärme- und Stoffübertragung.* 15: 255-270.
- Adamek, T., Webb, R.L. 1990. Prediction of film condensation on horizontal integral finned tubes. *Int. J. Heat Mass Transfer.* 33 (3): 1721-1735.
- Beatty, K.O., Katz, D.K. 1948. Condensation of vapors on outside of finned tubes, *Chem. Engineering Progress.* 44 (1): 55-70.
- Belghazi, M., Signe, J.C., Bontemps, A., Marvillet, C. 1998. Filmwise condensation of R134a and R23/R134a mixture on horizontal finned tubes. Influence of fin spacing. *Proc. Eurotherm 62, Heat transfer in condensation and evaporation.* 466-475. Grenoble, France, 17-18 November.
- Belghazi, M. 2001. Condensation d'un fluide pur et de mélanges zéotropes à l'extérieur d'un faisceau de tubes à surface améliorée, (Condensation heat transfer of a pure fluid and zeotropic mixtures outside a bundle of enhanced horizontal tubes). Ph. D. Thesis, Université Joseph Fourier, Grenoble, France, (in French).
- Belghazi, M., Bontemps, A., Signe, J.C., Marvillet, C. 2001. Condensation heat transfer of a pure fluid and binary mixture outside a bundle of smooth horizontal tubes. Comparison of experimental results and a classical model. *Int. J. Refrigeration.* 24 (8): 841-855.
- Bell, K.J., Ghaly, M.A. 1973. An approximate generalized design method for multicomponent/partial condensers. *Trans. of ASME.* 69(131): 72-79.
- Blanc, P. 1994. Condensation des fluides frigorigènes HFC 134a et HCFC 22 à l'extérieur d'un faisceau de tubes améliorés, (Condensation of HFC 134a and HCFC 22 outside a bundle of enhanced tubes). Ph. D. Thesis, Université J. Fourier, Grenoble, France, (in French).
- Briggs, A., Rose, J.W. 1994. Effect of fin efficiency on a model for condensation heat transfer on a horizontal integral-fin tube. *Int. J. Heat Mass Transfer.* 37: 457-453.
- Briggs, A., Rose, J.W. 1999. An evaluation of models for condensation heat transfer on low-finned tubes. *J. Enhanced Heat Transfer.* 6: 51-60.
- Briggs, A., Huang, X., Rose, J.W. 1995. An experimental investigation of condensation on integral-fin tubes: effect of film thickness, height and thermal conductivity. *Nat. Heat Transfer Conf., ASME HTD.* 308: 21-29.
- Briggs, A., Rose, J. 1999. An evaluation of models for condensation heat transfer on low-finned tubes. *J. Enhanced Heat Transfer.* 6: 51-60.
- Browne, M.W., Bansal, P.K. 1999. An overview of condensation heat transfer on horizontal tube bundles. *Applied Thermal Engineering.* 19: 565-594.
- Butrimowicz, D., Trela, M. 1997. Investigation of heat transfer on a horizontal finned tube fitted with the drainage strip. *Archives of thermodynamics.* 18 (3-4): 25-48.

- Cavallini, A., Doretto, L., Longo, G.A., Rossetto, L. 1996. A new model for forced convection on integral-fin tubes. *Trans. ASME, J. Heat Transfer*. 118: 689-693.
- Chen, M.M. 1961. An analytical study of laminar condensation: Part 2, Single and multiple horizontal tubes. *Trans. ASME, J. Heat Transfer*. 83: 55-60.
- Cheng, B., Tao, W.Q. 1994. Experimental study of R-152a film condensation on single horizontal smooth tube and enhanced tubes. *Trans. ASME, J. Heat Transfer*. 116: 256-270.
- Cheng, W.Y., Wang, C.-C. 1994. Condensation of R134a on enhanced tubes. *ASHRAE Transactions: Symposia*. 94-10-1: 809-817.
- Chilton, T.H., Colburn, A.P. 1934. Mass transfer coefficients prediction from data on heat transfer and fluid friction. *Ind. Engineering Chem*. 26: 1183-1187.
- Colburn, A.P., Hougen, O.A. 1934. Design of cooler condensers for mixtures of vapors with non-condensing gases. *Ind. Engineering Chem*. 26 (11): 1178-1182.
- Colburn, A.P., Drew, T.B. 1937. The condensation of mixed vapors, *Trans. A.I.Ch.E.* 33: 197-215.
- Collier, J.G., Thome, J.R. 1994. *Convective boiling and condensation*, Oxford Univ. Press.
- Das, A.,K., Meyer, G.A., Incek, G.A., Marto, P.J., Memory, S.B. 1995. Effects of fin height and thermal conductivity on the performance of integral-fin tubes for steam condensation. *Nat. Heat Transfer Conf., ASME HTD*. 308: 111-122.
- Denny, V. E., South III, V. 1972. Effects of forced flow, noncondensable and variable properties on film condensation of pure and binary vapors at the forward stagnation point of a horizontal cylinder. *Int. J. Heat Mass Transfer*. 15: 2133-2141.
- Fujii, T., Koyama, Sh., Ndiwalana, N.M., Nakamura, Y. 1990. Experimental study of gravity controlled condensation of binary vapor mixtures on a smooth horizontal tube, *Proc. 9th Int. Heat Transfer Conf.*, Jerusalem. 3: 109-114.
- Gregorig, R. 1954. Film condensation on finely rippled surfaces with consideration of surface tension. *Z. Angew. Math. Phys.* 5: 36-49.
- Hijikata, K., Himeno, N. 1986. Free convective filmwise condensation of a binary mixture of vapors, *Proc. 8th Int. Heat Transfer Conf.*, San Francisco, 4: 1621-1626.
- Hijikata, K., Himeno, N. 1990. Condensation of azeotropic and non-azeotropic binary vapor mixtures. in *Annual Review of Heat Transfer*. 3 (Ch. 2): 39-83.
- Hijikata, K., Himeno, N., Goto, S. 1990. Forced convective condensation of nonazeotropic binary mixture on vertical and horizontal tubes. *Proc. 9th Int. Heat Transfer Conf.*, Jerusalem. 4: 271-276.
- Honda, H., Makishi, O. 1995. Effect of circumferential rib on film condensation on a horizontal two-dimensional fin. *J. Enhanced Heat Transfer*. 2 (4): 307-315.
- Honda, H., Nozu, S., Mitsumori, K. 1983. Augmentation of condensation on horizontal finned tubes by attaching a porous drainage plate. *Proc. ASME-JSME Thermal Engng Joint Conference*, Honolulu (ed. Y. Mori and Y.J. Yang). 3: 289-296.
- Honda, H., Nozu, S. 1987. A prediction method for heat transfer during film condensation on horizontal low integral-fin tubes. *J. Heat Transfer*. 108: 218-225.

- Honda, H., Nozu, S., Uchima, B. 1987. A generalised prediction method for heat transfer during film condensation on a horizontal low finned tube. *Proc. 2nd ASME-JSME Thermal Engineering Joint Conference* (eds. P.J. Marto and I. Tanasawa). 4: 385-392.
- Honda, H., Nozu, S., Takeda, Y. 1989. A theoretical model of film condensation in a bundle of horizontal low finned tubes. *ASME, J. Heat Transfer*. 11: 525-532.
- Honda, H., Uchima, B., Nozu, S., Nakata, H., Torigoe, E. 1991. Film condensation of R-113 on in-line bundles of horizontal finned tubes. *ASME, J. Heat Transfer*. 113: 479-486.
- Honda, H., Uchima, B., Nozu, S., Nakata, H., Torigoe, E., Imai, S. 1992. Film condensation of R-113 on staggered bundles of horizontal finned tubes. *ASME, J. Heat Transfer*. 114: 442-449.
- Honda, H., Takamatsu, H., Takata, N. 1999. Experimental measurements for condensation of downward-flowing R123/R134a in a staggered bundle of horizontal low-finned tubes with four geometries. *Int. J. Refrigeration*. 22: 615-624.
- Karkhu, V.A., Borovkov, V.P. 1971. Film condensation of vapor at finely-finned horizontal tubes. *Heat Transfer - Soviet Research*. 3 (2): 183-191.
- Katz, D.L., Geist, J.M. 1948. Condensation of six finned tubes in a vertical row. *Trans. ASME, J. Heat Transfer*. 70: 907-914.
- Kedierski, M.A., Webb, R.L. 1990. Practical fin shapes for surface-tension-drained condensation. *ASME J. Heat Transfer*. 112: 479-485.
- Kern, D.Q. 1965. in *Process Heat Transfer*. Mc Graw Hill, New York.
- Kuang, L., Chen, Z. 1985. An experimental investigation for condensation of non-azeotropic refrigerant mixtures outside a horizontal tube. *Proc. 2nd Symp. on Multiphase Flow and Heat Transfer*. Xian, China. pp. 585-593.
- McNaught, J. M. 1979. Mass-transfer correction terms in design methods for multi-component/partial condensers. Condensation heat transfer. *18th Nat. Heat Transfer Conf.*, San Diego. New York ASME, 111-118.
- Marto, P.J. 1984. Heat transfer and two-phase flow during shell-side condensation. *Heat Transfer Engineering*. 5 (1-2): 31-61.
- Marto, P.J. 1986. Recent progress in enhancing film condensation heat transfer on horizontal tubes. *Proc. 8th Int. Heat Transfer Conf.* 1: 161-170.
- Marto, P.J., Mitrou, E., Wanniarachchi, A.S., Rose, J.W. 1986. Film condensation of steam on horizontal finned tubes: Effect of fin shape. *Proc. 8th Int. Heat Transfer Conf.* 4: 1695-1700.
- Marto, P.J. 1988. An evaluation of film condensation on horizontal integral fin tubes. *ASME J. Heat Transfer*. 110 (4 B): 1287-1305.
- Masuda, H., Rose, J. 1987. Static configuration of liquid films with low radial fins: implications for condensation heat transfer. *Proc. R. Soc. Lond.* A410: 125-139.
- Michael, A.G., Marto, P.J., Wanniarachchi, A.S., Rose, J.W. 1990. Filmwise condensation of R-113 on horizontal integral-fin tubes of different diameters. *Proc. 9th Int. Heat Transfer Conf.*, Jerusalem. 3: 15-20.
- Murata, K., Hashizume, C.G. 1992. Prediction of condensation heat transfer coefficient in integral-fin tube bundles. *Exp. Heat Transfer*. 5: 115-130.

- Murphy, R.W., Chen, F. C., Hwang, B. C. 1988. Condensing heat transfer for R114/R12 mixtures on horizontal finned tubes. *Revue Int. du Froid*. 11: 361-366.
- Nusselt, W. 1916. Die Oberflächen Kondensation der Wasserdampfes. *VDI Zeitung*. 60: 541-546, 569-575.
- Owen, R.G., Sardesai, R.G., Smith, R.A., Lee, W.C. 1983. Gravity controlled condensation on low integral-fin tubes. *Proc. Symp. on Condensers: Theory and practice, I. Chem. Symp. Ser. No. 75*, pp. 415-428.
- Rifert, V. 1998. Condensation on profiled surfaces - 50 years of theoretical and experimental researches, Eurotherm 62 *Proc. Heat transfer in condensation and evaporation*, pp. 476-488, Grenoble, France, 17-18 November.
- Rohsenow, W.M. 1956. Heat transfer and temperature distribution in laminar film condensation. *Trans. ASME*. 78 (8): 1645-1648.
- Rose, J.W. 1994. An approximate equation for the vapour-side heat transfer coefficient for condensation on low-finned tubes. *Int. J. Heat Mass Transfer*. 37 (5): 865-875.
- Rose, J.W., Uehara, H., Koyama, S., Fujii, T. 1999. Film condensation, in *Handbook of phase change*, (eds. Kandlikar, S.G., Shoji, M., Dhir, V.K.), Taylor & Francis, Philadelphia.
- Rudy, T.M., Webb, R.L. 1981. Condensate retention on horizontal integral-fin tubing. *Advances in heat transfer, ASME HTD*. 18: 34-41.
- Rudy, T.M., Webb, R.L. 1985. An analytical model to predict condensate retention on horizontal integral-fin tubes. *J. Heat Transfer*. 107: 361-368.
- Sami, S. M., Schnotale, J. 1992. Prediction of two phase flow condensation of pure and refrigerant mixtures on enhanced surface tubing. *Int. Comm. Heat Mass Transfer*. 19 (2): 191-202.
- Sardesai, R.G., Owen, R.G., Smith, R.A. 1982. *AERE Report 10619*.
- Shah, R.K., Zhou, S.Q., Tagavi, K.A. 1999. The role of surface tension in film condensation in extended surface passages. *Enhanced Heat Transfer*. 6: 179-216.
- Signe, J.C., Bontemps, A., Marvillet, C. 1998. Condensation heat transfer of a pure fluid and binary mixture in a bundle of smooth horizontal tubes. Comparison of experimental results and classical models. *Proc. Eurotherm 62, Heat transfer in condensation and evaporation*. 445-455. Grenoble, France, 17-18 November.
- Silver, L. 1947. Gas cooling with aqueous condensation. *Trans. Inst. Chem. Eng.* 25: 30-42.
- Smirnov, G.F., Lukanov, I.I. 1972. Study of heat transfer from freon 11 condensing on a bundle of finned tubes. *Heat Transfer - Soviet Research*. 4 (3): 51-56.
- Sparrow, E.M., Gregg, J.L. 1959. Laminar condensation heat transfer on a horizontal cylinder, *Trans. ASME*. 81: 13-18.
- Sreepathi, L.K., Bapat, S.L., Sukhatme, S.P. 1996. Heat transfer during film condensation of R-123 vapour on horizontal integral-fin tubes. *Journal of Enhanced Heat Transfer*. 3 (2): 147-164.
- Sukhatme, S.P. 1990. Condensation on enhanced surface horizontal tubes. *Proc. 9th Int. Heat Transfer Conf.*, Jerusalem. 1: 305-328.
- Thome, J.R. 1994. Two-phase heat transfer to new refrigerants. *Proc. 10th Int. Heat Transfer Conf.*, Brighton, 1: 19-41.

- Wanniarachchi, A.S., Marto, P.J., Rose, J.W. 1985. Film condensation of steam on horizontal finned tubes: effect of fin spacing, thickness and height. *ASME HTD, Multiphase heat transfer*. 47: 93-99.
- Wanniarachchi, A.S., Marto, P.J., Rose, J.W. 1986. Film condensation of steam on horizontal finned tubes: effect of fin spacing. *ASME HTD*. 108: 960-966.
- Wang, S.-P., Chato, J.C. 1995. Review of recent research on heat transfer with mixtures - Part I: Condensation. *ASHRAE Trans*. 101 (1): 1376-1386.
- Wang, W.C., Yu, C., Wang, B.X. 1995. Condensation heat transfer of a non-azeotropic binary mixture on a horizontal tube. *Int. J. Heat Mass Transfer*. 38 (2): 233-240.
- Webb, D. R. 1996. Future needs and developments in heat exchanger technology. Condensation. *Com. to Heat exchange engineering. European research meeting*. Birmingham, UK.
- Webb, D. R., Fahrner, M., Schwaab, R. 1996. The relationship between the Colburn and Silver methods of condenser design. *Int. J. Heat Mass Transfer*. 39 (15): 3147-3156.
- Webb, R.L., Keswani, S.T., Rudy, T.M. 1982. Investigation of surface tension and gravity effects in film condensation. *Proc. Int. Heat Transfer Conference*, Washington. 5: 175-180.
- Webb, R.L., Rudy, T.M., Kedzierski, M.A. 1985. Prediction of condensation coefficient on horizontal integral-fin tubes. *ASME J. Heat Transfer*. 107: 369-376.
- Webb, R.L. 1988. Enhancement of condensation. *Int. Comm. Heat Mass Transfer*. 15 (4): 475-507.
- Webb, R.L., Murawski, C.G. 1990. Row effect for R-11 condensation on enhanced tube. *ASME J. Heat Transfer*. 112: 768-776.
- Yang, C.-Y. 1999. A critical review of condensation heat transfer predicting models - Effects of surface-tension force. *Enhanced Heat Transfer*. 6: 217-236.
- Zhu, H.R., Honda, H. 1993. Optimisation of fin geometry of a horizontal low-finned condenser tube. *Heat Transfer-Jap. Res.* 22 (4): 372-386.